Gradient damage models coupled with plasticity: Variational formulation and main properties

Roberto Alessi, Jean-jacques Marigo, Stefano Vidoli

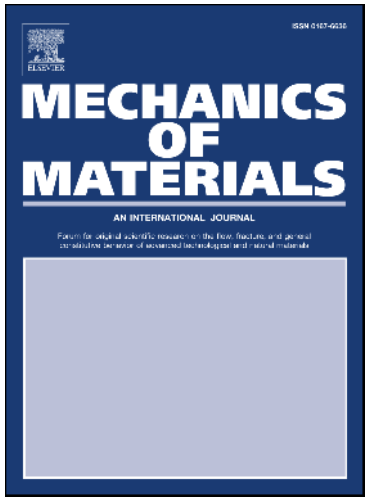

Gradient damage models coupled with plasticity: variational formulation and main properties

Roberto Alessi, Jean-Jacques Marigo, Stefano Vidoli

PII: S0167-6636(14)00003-9
DOI: http://dx.doi.org/10.1016/j.mechmat.2013.12.005
Reference: MECMAT 2226

To appear in: *Mechanics of Materials*

Please cite this article as: Alessi, R., Marigo, J-J., Vidoli, S., Gradient damage models coupled with plasticity: variational formulation and main properties, *Mechanics of Materials* (2014), doi: http://dx.doi.org/10.1016/j.mechmat.2013.12.005

Gradient damage models coupled with plasticity: variational formulation and main properties

Roberto Alessi[a,c], Jean-Jacques Marigo[*,c], Stefano Vidoli[a,b]

[a] *Dipartimento di Ingegneria Strutturale e Geotecnica, Sapienza Università di Roma, Via Eudossiana 18, 00184 Roma, Italy*
[b] *Institut Jean Le Rond D'Alembert, UPMC, Paris, France*
[c] *Laboratoire de Mécanique des Solides, Ecole Polytechnique, 91128 Palaiseau Cedex, France*

Abstract

A variational formulation is proposed for a family of elastic-plastic-damage models within the framework of rate-independent materials. That consists first in defining the total energy which contains, in particular, a gradient damage term and a term which represents the plastic dissipation but depends also on damage. Then, the evolution law is deduced from the principles of irreversibility, stability and energy balance. Accordingly, the plastic dissipation term which appears both in the damage criterion and the plastic yield criterion plays an essential role in the damage-plasticity coupling. Suitable constitutive choices on how the plastic yield stress decreases with damage, allows us to obtain a rich variety of coupled responses. A particular attention is paid on the equations which govern the formation of cohesive cracks where the displacement is discontinuous and the plasticity localizes. In the one-dimensional traction test where the solution is obtained in a closed form, we show that, because of damage localization, a cohesive crack really appears at the center of the damage zone before the rupture and the associated cohesive law is obtained in closed form in terms of the constitutive parameters. A Finite Element discrete version of the energy functional is used to simulate a two-dimensional traction test over a rectangular domain with mixed boundary conditions; again a localized band of plastic strain is generated seemingly independent of the mesh size.

Key words: gradient damage model, cohesive crack, plasticity, variational approach, ductile fracture

1. Introduction

Gradient damage models are very efficient to account for the behavior of brittle and quasi-brittle materials. Such models have been developed independently by different group of authors, see for instance Peerlings et al. (1998); Comi (1999); Bourdin et al. (2000); Comi et al. (2006); Benallal and Marigo (2007); Pham and Marigo (2010a,b); Lorentz et al. (2011). Their main merit is that they are able to account for both the nucleation and the propagation of cracks in a unified framework. Their basic ingredients are: (i) a decreasing dependency of the stiffness $\mathtt{E}(\alpha)$ on the damage variable α; (ii) no more rigidity at the ultimate damage state (say $\mathtt{E}(1) = 0$); (iii) a critical stress σ_c; (iv) a softening behavior with a decrease of the stress from σ_c to 0 when the damage goes to 1; (v) a gradient damage term in the energy which necessarily contains an internal length ℓ and which limits the damage localization.

Accordingly, it can be shown in a one-dimensional setting that the process of crack nucleation consists in the following three successive stages, see Pham et al. (2011a); Pham and Marigo (2013a); Sicsic et al. (2013): (i) first, damage occurs in a neighborhood of a point where the stress reaches the material critical stress; (ii) then, damage grows inside a damage zone the width of which is related to the material characteristic length ℓ; (iii) finally, damage reaches the critical value 1 at the center of the damage zone and a crack

*Corresponding author
Email addresses: roberto.alessi@uniroma1.it (Roberto Alessi), marigo@lms.polytechnique.fr (Jean-Jacques Marigo), stefano.vidoli@uniroma1.it (Stefano Vidoli)

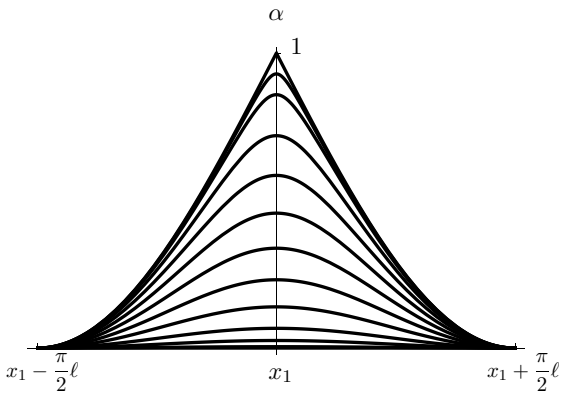

Figure 1: In one-dimension, nucleation of a crack at the center x_1 of a damage zone of width $\pi\ell/2$, ℓ being the material characteristic length. The graphs represent the growth of the damage field with time. At final time $\alpha(x_1) = 1$, a crack has appeared at x_1.

appears at this point, see Fig. 1. During this crack nucleation process, some energy is dissipated inside the damage zone and this dissipated energy involves a quantity $\mathsf{G_c}$ which can be considered as the effective surface energy of Griffith's theory. Therefore, $\mathsf{G_c}$ becomes a byproduct of the gradient damage model which can be expressed in terms of the parameters of the model (specifically, $\mathsf{G_c}$ is proportional to $\sigma_c^2\ell/\mathtt{E}(0)$ Pham and Marigo (2013a)).

In two or three dimensions, the process of crack nucleation essentially follows the same stages. For example, in Fig. 2 are illustrated in a two-dimensional setting these different phases of nucleation and propagation of an array of cracks which are obtained by this type of gradient damage model in the case of a thermal shock, see Sicsic et al. (2013) for details. Moreover, once a crack has nucleated, it can be proved Sicsic and Marigo (2013) that its propagation is essentially governed by Griffith's law, *i.e.* the law based on the concept of critical energy release rate criterion where the role of the critical energy release rate is played by the dissipated energy density $\mathsf{G_c}$.

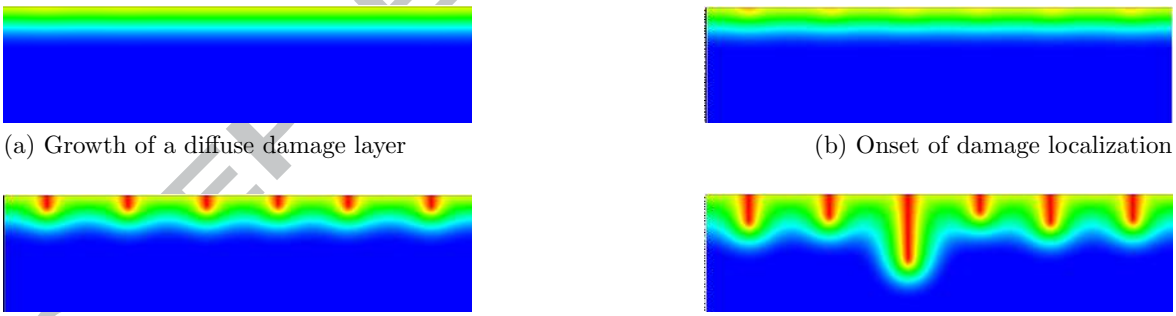

(a) Growth of a diffuse damage layer

(b) Onset of damage localization

(c) Nucleation of periodically spaced cracks

(d) Propagation and arrest of cracks

Figure 2: Numerical simulation by a gradient damage model of the damage evolution during the thermal shrinking induced by cooling through the top surface of the sample Sicsic et al. (2013). In blue, the sound material; in red, the totally damaged material.

However, this type of "quasi-brittle" models are not able to account for residual strains and consequently cannot be used in the case where the fracture occurs with a significant plastic zone. Moreover there is no discontinuity of the displacement in the damage strip before the loss of rigidity at its center, *i.e.* before the nucleation of a crack. In other words such a model cannot account for the nucleation of cohesive cracks, *i.e.* the existence of surface of discontinuity of the displacement with a non vanishing stress. The natural way to include such effects is to introduce plastic strains into the model and to couple their evolution with

damage evolution. Of course, this idea is not new and a great number of damage models coupled with plasticity have been developed from the eighties in the spirit of Lemaitre and Chaboche (1985), see for instance de Borst et al. (1999); Grassl and Jirásek (2006); Belnoue et al. (2007); Dimitrijevic and Hackl (2011). But our purpose is to construct such models in a softening framework with gradient of damage terms and to see how these models can account for the nucleation of cracks in presence of plasticity. In our knowledge, the previous works are not able to go so far. Such regularization methods by adding gradient terms also exist for other types of behavior exhibiting strain-softening. It is not possible to quote here all the abundant literature devoted to this topic and it is not the goal of the present paper to compare all or a part of these approaches with ours. The reader interested by such a comparison should refer to Lorentz and Andrieux (2003) where a general overview was proposed, or to the more recent work Dal Corso and Willis (2011) where a regularization by gradient plastic strain is proposed for elastic-plastic (but non damaging) materials. Let us simply remark that none of the quoted works are able to treat in a unified manner the delicate issue of nucleation of cohesive and non cohesive cracks.

Here we will adopt a variational approach in the spirit of previous works Mielke (2005, 2006); Bourdin et al. (2008); Del Piero and Truskinovsky (2009); Pham and Marigo (2010a,b); Pham et al. (2011a); Sicsic and Marigo (2013); Del Piero (2013). Such an approach is fundamental both from the theoretical and numerical viewpoints. From the theoretical viewpoint, that allows us to construct the model in a rational and systematic way. Indeed, the main steps are the following ones: (i) one defines the total energy of the body in terms of the state fields which include the displacement field and the internal variable fields, namely the damage, the plastic strain and the cumulated plastic strain fields; (ii) one postulates that the evolution of the internal variables is governed by the three general principles of *irreversibility*, *stability* and *energy balance*. Besides, we have the chance that the variational approach works and has been already developed both in plasticity and in damage mechanics, even though only separately up to now. So, it "suffices" to introduce the coupling by choosing the form of the total energy to obtain, by virtue of our plug and play device, a model of gradient damage coupled with plasticity: the damage and plasticity criteria are deduced from the stability principle; the normality flow rule for the plastic strain has not to be postulated but is a consequence of the stability principle and the energy balance; we derive new jump conditions and another normality flow rule on a surface of discontinuity (shear band or cohesive crack). In this paper, our choice of coupling is minimalist in the sense that it simply consists in introducing the dependence of the yield plastic stress $\sigma_{\mathsf{p}}(\alpha)$ on the damage variable (with the natural assumption that $\sigma_{\mathsf{p}}(\alpha)$ goes to 0 when the damages goes to 1). In turn, by virtue of the variational character of the model, the product $\sigma_{\mathsf{p}}'(\alpha)\bar{p}$ of the derivative of the state function $\sigma_{\mathsf{p}}(\alpha)$ by the cumulated plastic strain $\bar{p}$ enters in the damage criterion and this coupling plays a fundamental role in the nucleation of a cohesive crack.

From the numerical viewpoint, the variational approach allows us to use an alternate minimization algorithm to solve the incremental evolution problem. This type of algorithm is used for a long time in plasticity and more recently in damage mechanics Bourdin et al. (2000). In the present context, it consists in minimizing at a given time step the total energy of the body alternatively with respect to one of the three state fields (displacement, plastic strain or damage field), the other two being fixed, and to iterate until convergence. It turns out that such an algorithm is automatically an algorithm of descent of the energy, what is very interesting to obtain a final state which satisfies the stability condition. It is this algorithm which allowed us to obtain the numerical results for the thermal shock problem plotted in Figure 2 and it will be used here in Sect. 5 to solve numerically the uniaxial traction problem.

Specifically, the paper is organized as follows. In Sect. 2 the energy and dissipation functionals of the model are presented; the main hypotheses on their constitutive functions are discussed and the explicit form of the balance and consistency equations, as dictated by the stability condition and by the energy balance, are explicitly stated. To model plastic effects we choose the simple framework of Von Mises plasticity criterion (more complex choices in this respect could be also considered). Once stated the governing equations, the homogeneous responses are studied in Sect. 3, by requiring all the fields to do not depend on the space variable. Three different responses are enlightened which corresponds to all basic kinds of coupling between the evolution of damage and plasticity. This classification guides also the study of non-homogeneous solutions in Sect. 4 and Sect. 5. Indeed it turns out that the homogeneous responses are not stable if the size of the domain is larger than a threshold; hence we are led to study the conditions under which

localization of both the damage and the plastic strain fields can occur. The interplay between damage and accumulated plastic strain is, for the case of non-homogeneous solutions, much richer: in some cases the model dictates the formation of a plastic hinge where the accumulated plastic strain must localize and the damage profile derivative, as well as the displacement field, suffers a jump. Sect. 4 is devoted to the standard one-dimensional traction test; in this case we are able to compute in closed form the nucleation of cohesive cracks and the associated, Barenblatt-type, cohesive law between the stress and the displacement jump. The two-dimensional analysis described in Sect. 5 requires instead a numerical implementation of the presented model. To this aim a Finite Element discrete version of the variational problem is implemented within the Fenics framework (Logg et al., 2012). Whilst for the one-dimensional traction test the code allows to recover the discussed analytic solution, a traction test problem over a rectangular material domain in plane-strain enlighten the formation of a 45° shear band and the necking of the specimen. Despite the localization phenomena occurring, these results are shown to be mesh-independent.

Notation. Throughout the paper, the following notations are used. N denotes the dimension of the space, $1 \leq N \leq 3$, $N = 1$ corresponds to the one-dimensional case and $N > 1$ to the multi-dimensional case. In the multi-dimensional case, vectors and second order tensors are denoted by boldface letters, e.g., $\mathbf{u}$ for the displacement and $\boldsymbol{\sigma}$ for the stress. Their components are denoted by the respective italic letters with lower indices like u_i or σ_{ij}, $1 \leq i, j \leq N$. The second order identity tensor is denoted $\mathbf{I}$. Fourth order tensors are denoted with typewriter letters, like $\mathtt{E}$ and $\mathtt{C}$ for the stiffness and compliance tensors respectively. The summation convention is implicitly used. The inner product between vectors or between second order tensors is indicated by a dot. Accordingly, one reads $\mathbf{u} \cdot \mathbf{v} = u_i v_i$, $\boldsymbol{\varepsilon} \cdot \boldsymbol{\varepsilon} = \varepsilon_{ij}\varepsilon_{ij}$, $\mathtt{E}\boldsymbol{\varepsilon} \cdot \boldsymbol{\varepsilon} = \mathtt{E}_{ijkl}\varepsilon_{ij}\varepsilon_{kl}$. The euclidean norm of a vector or a second order tensor is denoted $\|\cdot\|$ and thus $\|\mathbf{u}\| = \sqrt{\mathbf{u} \cdot \mathbf{u}}$. The trace operator for a second order tensor is denoted Tr and thus $\operatorname{Tr} \mathbf{p} = \mathbf{p} \cdot \mathbf{I} = p_{ii}$. The deviatoric operator is represented by the superscript D and thus $\boldsymbol{\sigma}^D$ denotes the deviatoric part of $\boldsymbol{\sigma}$, *i.e.*

$$\boldsymbol{\sigma}^D = \boldsymbol{\sigma} - \frac{\operatorname{Tr} \boldsymbol{\sigma}}{N} \mathbf{I}.$$

The dependence on the time parameter t is indicated by a subscript whereas the dependence on the spatial coordinate $\mathbf{x}$ is indicated classically by parentheses, e.g. $\mathbf{x} \mapsto \mathbf{u}_t(\mathbf{x})$ stands for the displacement field at time t. In general, the state functions or the material parameters are represented by sans serif letters, like Y_0 for the Young modulus, d_1 for the local dissipated energy by damage or $\mathsf{w}(\alpha)$ for the damage change of variable. The prime denotes either the derivative with respect to the spatial coordinate x in a one-dimensional setting or the derivative with respect to the damage parameter, the dot stands for the time derivative, e.g.

$$u_t'(x) = \frac{du_t}{dx}(x), \quad \mathtt{E}'(\alpha) = \frac{d\mathtt{E}}{d\alpha}(\alpha), \quad \dot{\mathbf{u}}_t(\mathbf{x}) = \lim_{h \to 0} \frac{1}{h}\Big(\mathbf{u}_{t+h}(\mathbf{x}) - \mathbf{u}_t(\mathbf{x})\Big).$$

The symbols ∇ and ∇_s will be respectively used to indicate the spatial gradient and its symmetric part when this last makes sense. Accordingly, the total strain tensor field reads as $\boldsymbol{\varepsilon} = \nabla_s \mathbf{u}$. Table 1 summarizes the main nomenclature used in this article.

State variables and state functions	
α	Scalar damage variable
$\omega = \mathsf{w}(\alpha)$	Change of damage variable used in the particular family of damage models
$\nabla\alpha$	Gradient of damage
$\boldsymbol{\varepsilon}$	Total strain tensor
$\mathbf{p}$	Plastic strain tensor
$\bar{p}$	Cumulated plastic strain
$\mathtt{E}(\alpha)$	State function giving the stiffness tensor
$\mathtt{C}(\alpha)$	State function giving the compliance tensor
$\mathsf{d}(\alpha)$	State function giving the energy density dissipated by damage
$\sigma_{\mathsf{D}}(\alpha)$	State function giving the damage critical stress
$\sigma_{\mathsf{P}}(\alpha)$	State function giving the plastic yield stress
$\mathsf{W}(\boldsymbol{\varepsilon}, \alpha, \nabla\alpha, \mathsf{p}, \bar{p})$	State function giving the strain work density

Material constants	
Y_0, ν_0	Young modulus and Poisson ratio of the undamaged material
d_1	Energy density dissipated by a fully damaged material point
$\bar{\sigma}_{\mathsf{D}} = \sigma_{\mathsf{D}}(0)$	Initial damage critical stress
$\bar{\sigma}_{\mathsf{P}} = \sigma_{\mathsf{P}}(0)$	Initial plastic yield stress
ℓ	Material characteristic length
G_{c}	Effective surface energy density

Space and time variables or fields	
N	Dimension of the space
Ω	Reference configuration of the N-dimensional body
$\partial_D\Omega$	Part of the boundary where the displacements are prescribed
$\partial_F\Omega$	Part of the boundary where the surface forces are prescribed
$\mathbf{x} = (x_1, \cdots, x_N)$	Material point and its cartesian coordinates in the reference configuration
t	Time variable
$\mathbb{M}_s^N$	Space of symmetric second order tensors in a N-dimensional setting
$\mathbf{u}$	Real displacement field
$\boldsymbol{\xi} = (\mathbf{u}, \alpha, \mathbf{p}, \bar{p})$	Real state field of the body
$J(\boldsymbol{\xi})$	Surface where the state field is singular
$[\![\mathbf{u}]\!]$	Jump discontinuity of the displacement field
$\mathbf{p}^R, \bar{p}^R$	Regular parts of the plastic strain and cumulated plastic strain fields
$\bar{P}$	Surface density of the singular part of the cumulated plastic strain field
$\mathbf{q}, \mathbf{q}^R$	Virtual plastic strain field and its regular part
$J(\mathbf{v})$	Jump set of the virtual displacement field $\mathbf{v}$

Table 1: Main nomenclature

2. The gradient damage model coupled with plasticity

2.1. Definition of the total energy state function

For quasi-brittle materials, one uses gradient damage models which are defined by assuming that the energy density has the following form

$$\mathsf{W}_{\mathsf{D}}(\boldsymbol{\varepsilon}, \alpha, \nabla\alpha) = \frac{1}{2}\mathtt{E}(\alpha)\boldsymbol{\varepsilon}\cdot\boldsymbol{\varepsilon} + \mathsf{d}(\alpha) + \mathsf{d}_1\ell^2\nabla\alpha\cdot\nabla\alpha, \tag{1}$$

where $\boldsymbol{\varepsilon} \in \mathbb{M}_s^N$ is the strain tensor and α is a scalar characterizing the damage level in the material; respectively $\alpha = 0$ and $\alpha = 1$ mean a sound and a totally damaged material. Here $\mathtt{E}(\alpha)$ represents the material

stiffness tensor, supposed decreasing with the damage variable, $\mathsf{d}(\alpha)$ account for the energy dissipation due to damage, $\nabla\alpha$ denotes the gradient of damage and the gradient damage term, which necessarily introduces an internal length $\ell > 0$, is used to limit the damage localization. Note that W_D represents the *total* energy density, sum of the stored (and recoverable) elastic energy and the energy dissipated during the damage process. Such models are able to account for the nucleation of cracks in brittle and "quasi-brittle" materials. However, they are not able to account for residual strains and consequently cannot be used in ductile fracture. The natural way to include such effects is to introduce plastic strains and to couple their evolution with damage evolution.

Before to introduce the coupling between damage and plasticity, it is important to recall that the classical plasticity theory can also be formulated in a variational form (at least when the plastic flow rule follows the normality rule). For instance, in the case of Von Mises yield criterion, the total energy density reads as

$$\mathsf{W}_\mathsf{P}(\boldsymbol{\varepsilon}, \mathbf{p}, \bar{p}) = \tfrac{1}{2}\mathtt{E}\,(\boldsymbol{\varepsilon} - \mathbf{p}) \cdot (\boldsymbol{\varepsilon} - \mathbf{p}) + \sigma_\mathsf{p}\,\bar{p}, \tag{2}$$

where $\mathbf{p} \in \mathbb{M}^N_s$ denotes the plastic strain tensor and $\bar{p}$ the cumulated plastic strain. Their definition depends on the dimension of the space.

In the one-dimensional case, the plastic strain is a scalar and hence is simply denoted p whereas the cumulated plastic strain is defined by

$$\dot{\bar{p}} = |\dot{p}|.$$

In the multi-dimensional case we adopt the plastic incompressibility condition and hence $\mathbf{p}$ is assumed to be purely deviatoric, $\operatorname{Tr}\mathbf{p} = \mathbf{0}$. The cumulated plastic strain $\bar{p}$ is a scalar defined by

$$\dot{\bar{p}} = \sqrt{\frac{N-1}{N}}\,\|\dot{\mathbf{p}}\|.$$

Accordingly, all the cases can be synthesized by the following formula

$$\dot{\bar{p}} = k_N\,\|\dot{\mathbf{p}}\| \quad \text{with} \quad \operatorname{Tr}\mathbf{p} = 0 \text{ if } N > 1 \quad \text{and} \quad k_N = \begin{cases} 1 & \text{if } N = 1 \\ \sqrt{\frac{N-1}{N}} & \text{otherwise} \end{cases}. \tag{3}$$

In (2), the fourth tensor $\mathtt{E}$ is the (invariable) stiffness tensor and the material constant σ_p represents the Von Mises yield stress. Hence, the first term represents the stored elastic energy and the second the energy dissipated during the plasticity process.

To couple damage with plasticity, we first define the state of a volume element by the quintuple $(\boldsymbol{\varepsilon}, \alpha, \nabla\alpha, \mathbf{p}, \bar{p}) \in \mathbb{M}^N_s \times [0,1] \times \mathbb{R}^N \times \mathbb{M}^N_s \times \mathbb{R}^+$ and then define the total energy density as the following function of state:

$$\mathsf{W}(\boldsymbol{\varepsilon}, \alpha, \nabla\alpha, \mathbf{p}, \bar{p}) = \tfrac{1}{2}\mathtt{E}(\alpha)(\boldsymbol{\varepsilon} - \mathbf{p}) \cdot (\boldsymbol{\varepsilon} - \mathbf{p}) + \mathsf{d}(\alpha) + \mathsf{d}_1\ell^2\nabla\alpha \cdot \nabla\alpha + \sigma_\mathsf{p}(\alpha)\,\bar{p}. \tag{4}$$

The definition (1) of the energy density has been altered by introducing the plastic strain field $\mathbf{p}$ in the stored elastic energy, and by adding the dissipation due to plastic deformations, namely $\sigma_\mathsf{p}(\alpha)\,\bar{p}$. Our choices in (4) are minimalist in the sense that

(i) the damage variable is still a scalar and one does not introduce another internal variable than the cumulated plastic strain in the dissipated energy state function. At this purpose, let us note that the most used models in ductile fracture by the engineering community, like Gurson-like models, contain also only one damage variable, namely the microvoid porosity;

(ii) for $\alpha = 0$ we are actually considering the standard Von Mises model of perfect plasticity. But there is no difficulty to change the shape of the plasticity criterion and more complex choices will be considered in the future;

(iii) the coupling between damage and plasticity simply consists in introducing a dependence of the yield plastic stress $\sigma_{\mathsf{P}}(\alpha)$ on the damage variable. Despite this simplicity and by virtue of the variational character of the model, we will see that the product $\sigma'_{\mathsf{P}}(\alpha)\bar{p}$ of the derivative of the state function $\sigma_{\mathsf{P}}(\alpha)$ by the cumulated plastic strain $\bar{p}$ enters in the damage criterion and this coupling will play a fundamental role in the onset of damage by plastic accumulation or in the nucleation of a cohesive crack at the center of a damage zone.

2.2. The total energy functional for a N-dimensional body

In (4), W denotes the energy of the volume element. Let us now consider a N-dimensional continuum body whose reference configuration is the open bounded domain Ω and which is submitted to a time-dependent loading process characterized by time-dependent surface forces $\mathbf{F}_t$ prescribed on the part $\partial_F\Omega$ of the boundary of Ω and by time-dependent displacements $\mathbf{U}_t$ prescribed on the complementary part $\partial_D\Omega = \partial\Omega \setminus \partial_F\Omega$. (To simplify the presentation, we will neglect body forces.) Then, at a given time t, the total energy of the body is the following functional of the quadruple

$$\boldsymbol{\xi} = (\mathbf{u}, \alpha, \mathbf{p}, \bar{p})$$

called the global state field, made of the displacement field $\mathbf{u}$, the damage field α, the plastic strain field $\mathbf{p}$ and the cumulated plastic strain field $\bar{p}$:

$$\mathcal{E}_t(\mathbf{u}, \alpha, \mathbf{p}, \bar{p}) = \int_\Omega \mathsf{W}(\nabla_s\mathbf{u}(\mathbf{x}), \alpha(\mathbf{x}), \nabla\alpha(\mathbf{x}), \mathbf{p}(\mathbf{x}), \bar{p}(\mathbf{x}))\, d\mathbf{x} - \int_{\partial_F\Omega} \mathbf{F}_t(\mathbf{x}) \cdot \mathbf{u}(\mathbf{x})\, dS. \tag{5}$$

The above expression of the energy makes sense provided that the global state field $\boldsymbol{\xi}$ is smooth enough. Let us briefly discuss these questions of regularity.

1. As far as the damage field is concerned, the gradient term requires that $\alpha \in H^1(\Omega)$ so that the total energy be finite. Therefore, the damage field is continuous across any surface, but the gradient of damage can be discontinuous.
2. As far as the displacement and the plastic strain fields are concerned, in our perfect plasticity setting (at given damage) the elastic strain field $\nabla_s\mathbf{u} - \mathbf{p}$ only is regular so that the elastic energy be finite (it must belong to $L^2(\Omega)$). In such a setting, it is well known that plasticity can localize in shear bands. We will see that it is actually the case once the damage has appeared, because of the localization of damage induced by the softening character of the model.

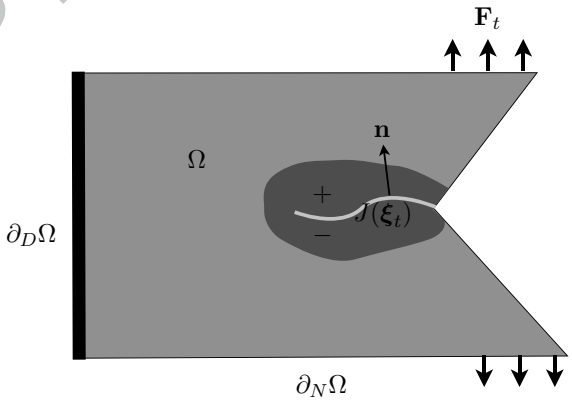

Figure 3: The N-dimensional body with its loading and the jump set $J(\boldsymbol{\xi}_t)$ of the current state field $\boldsymbol{\xi}_t$ (light grey curve) inside a plastic-damaged non singular zone (dark grey zone)

Accordingly, we will assume that the global state field $\boldsymbol{\xi} = (\mathbf{u}, \alpha, \mathbf{p}, \bar{p})$ is piecewise smooth and that its "singular part" is localized on a $\boldsymbol{\xi}$-dependent set $J(\boldsymbol{\xi}) \subset \Omega$, called the *jump set* of $\boldsymbol{\xi}$, which contains a finite

number of smooth and non-intersecting surfaces in Ω. For a sake of simplicity, we also assume that this set has zero intersection with the boundary $\partial\Omega$, see Fig. 3. Specifically, we assume that

(i) the displacement field $\mathbf{u}$ is continuously differentiable on $\Omega \setminus J(\boldsymbol{\xi})$ and admits a jump discontinuity on $J(\boldsymbol{\xi})$. Therefore, the strain field $\boldsymbol{\varepsilon}$ associated with $\mathbf{u}$ can be decomposed into two parts: its regular part $\boldsymbol{\varepsilon}^R$ which corresponds to the usual symmetric part of the gradient of $\mathbf{u}$ and its singular part which can be seen as a Dirac measure concentrated on the jump set $J(\boldsymbol{\xi})$. The singular part of $\boldsymbol{\varepsilon}$ is denoted by $\boldsymbol{\varepsilon}^S$ and is written with an abuse of notation as

$$\boldsymbol{\varepsilon}^S = [\![\mathbf{u}]\!] \otimes_s \mathbf{n}\ \delta_{J(\boldsymbol{\xi})}, \tag{6}$$

where $\mathbf{n}$ is the normal to the positive face of $J(\boldsymbol{\xi})$, $[\![\mathbf{u}]\!] := \mathbf{u}^+ - \mathbf{u}^-$ and δ_J is the Dirac surface measure concentrated on the surface J.

(ii) in order that the elastic energy be finite, the plastic strain field $\mathbf{p}$ has the same singular part as the strain field and hence its singular part $\mathbf{p}^S$ will also read as

$$\mathbf{p}^S = [\![\mathbf{u}]\!] \otimes_s \mathbf{n}\ \delta_{J(\boldsymbol{\xi})} \tag{7}$$

while its regular part (denoted $\mathbf{x} \mapsto \mathbf{p}^R(\mathbf{x})$) is assumed at least continuous on $\Omega \setminus J(\boldsymbol{\xi})$. In the multi-dimensional case, for $\mathbf{p}$ to be deviatoric its singular part must be such that $\mathrm{Tr}([\![\mathbf{u}]\!] \otimes_s \mathbf{n}) = [\![\mathbf{u}]\!] \cdot \mathbf{n} = 0$; hence in dimension higher than one, only the tangential components of the displacement can jump through $J(\boldsymbol{\xi})$.

(iii) in the same manner, the cumulated plastic strain field is decomposed into regular and singular parts $\bar{p}^R$ and $\bar{p}^S$. Its singular part reads as

$$\bar{p}^S = \bar{P}\ \delta_{J(\boldsymbol{\xi})} \tag{8}$$

and thus $\bar{P}$ denotes its surface density.

Finally, the total energy of the body in the global state $\boldsymbol{\xi} = (\mathbf{u}, \alpha, \mathbf{p}, \bar{p})$ will read as

$$\begin{aligned} \mathcal{E}_t(\mathbf{u}, \alpha, \mathbf{p}, \bar{p}) \;=\; & \int_{\Omega \setminus J(\boldsymbol{\xi})} \tfrac{1}{2}\mathbb{E}(\alpha(\mathbf{x}))\Big(\nabla_s \mathbf{u}(\mathbf{x}) - \mathbf{p}^R(\mathbf{x})\Big) \cdot \Big(\nabla_s \mathbf{u}(\mathbf{x}) - \mathbf{p}^R(\mathbf{x})\Big) d\mathbf{x} \\ & + \int_{\Omega \setminus J(\boldsymbol{\xi})} \Big(\mathtt{d}(\alpha(\mathbf{x})) + \sigma_{\mathtt{p}}(\alpha(\mathbf{x}))\bar{p}^R(\mathbf{x}) + \mathtt{d}_1 \ell^2 \nabla\alpha(\mathbf{x}) \cdot \nabla\alpha(\mathbf{x})\Big) d\mathbf{x} \\ & + \int_{J(\boldsymbol{\xi})} \sigma_{\mathtt{p}}(\alpha(\mathbf{x}))\bar{P}(\mathbf{x})\ dS - \int_{\partial_F \Omega} \mathbf{F}_t(\mathbf{x}) \cdot \mathbf{u}(\mathbf{x})\ dS. \end{aligned} \tag{9}$$

The only singular part which appears in (9) is that of the cumulated opening, because α and $\nabla\alpha$ are not singular whereas $\boldsymbol{\varepsilon}$ and $\mathbf{p}$ have the same singular part.

2.3. Damage irreversibility, local stability and energy balance

At this stage of the construction, nothing was said on the laws governing the evolution of the damage and the plasticity. One of the main advantages of the variational approach is that those laws are simple byproducts of the general physical principles of *irreversibility*, *stability* and *energy balance* once the total energy has been defined. These principles are briefly recalled below and the reader interested by more details can refer to Mielke (2005, 2006); Bourdin et al. (2008); Pham and Marigo (2010a,b); Francfort and Giacomini (2012). Then, this section and the Appendix will be devoted to the deduction of the damage and plasticity evolution laws from these three principles and the assumed form (9) of the energy.

2.3.1. The irreversibility condition

We require that at every point the damage can only increase with time, *i.e.*

$$\dot{\alpha}_t(\mathbf{x}) \geq 0, \qquad 0 \leq \alpha_t(\mathbf{x}) \leq 1, \quad \forall \mathbf{x} \in \Omega. \tag{10}$$

Moreover, to simplify the presentation, we will only consider the evolution before the nucleation of a full damaged set and hence we assume that $\alpha_t < 1$ everywhere in Ω.

2.3.2. Stability condition

Let $\boldsymbol{\xi}_t = (\mathbf{u}_t, \alpha_t, \mathbf{p}_t, \bar{p}_t)$ be the state of the body at time t and let $\boldsymbol{\xi}^* = (\mathbf{u}^*, \alpha^*, \mathbf{p}^*, \bar{p}^*)$ be the following virtual state

$$\boldsymbol{\xi}^* = \boldsymbol{\xi}_t + h\left(\mathbf{v}, \beta, \mathbf{q}, k_N\|\mathbf{q}\|\right)$$

where h is a positive constant. In order that $\mathbf{u}^*$ be kinematically admissible, the field $\mathbf{v}$ must be such that $\mathbf{v} = \mathbf{0}$ on $\partial_D\Omega$. Moreover, the field $\mathbf{v}$ is assumed, like $\mathbf{u}_t$, piecewise smooth and we denote by $J(\mathbf{v})$ the set of points where $\mathbf{v}$ is discontinuous. Therefore the jump set of $\boldsymbol{\xi}^*$ is $J(\boldsymbol{\xi}^*) = J(\boldsymbol{\xi}_t) \cup J(\mathbf{v})$. Finally the field $\mathbf{p}^*$ is admissible if, in the multi-dimensional case, $\operatorname{Tr}\mathbf{q} = 0$ and if the singular part of $\mathbf{q}$ is related to the jump of $\mathbf{v}$ by

$$\mathbf{q}^S = [\![\mathbf{v}]\!] \otimes_s \mathbf{n}\, \delta_{J(\mathbf{v})}. \tag{11}$$

In order that $\alpha_t \leq \alpha^* < 1$ and that $\alpha^* \in H^1(\Omega)$, it is necessary and sufficient that $\beta \geq 0$, $\beta \in H^1(\Omega)$ and h be small enough. A triple of fields $(\mathbf{v}, \beta, \mathbf{q})$ which satisfies the above conditions will be called an admissible direction of perturbation. We are now in a position to define the condition of stability.

Definition (Local stability)**.** *The state $(\mathbf{u}_t, \alpha_t, \mathbf{p}_t, \bar{p}_t)$ of the body at a time t before the nucleation of a crack is said locally stable if, for every admissible direction of perturbation $(\mathbf{v}, \beta, \mathbf{q})$, there exists $\bar{h} > 0$ such that for all $h \in [0, \bar{h}]$*

$$\mathcal{E}_t\Big(\mathbf{u}_t + h\mathbf{v}, \alpha_t + h\beta, \mathbf{p}_t + h\mathbf{q}, \bar{p}_t + hk_N\|\mathbf{q}\|\Big) \geq \mathcal{E}(\mathbf{u}_t, \alpha_t, \mathbf{p}_t, \bar{p}_t). \tag{12}$$

2.3.3. Energy balance

Following the presentation of Pham and Marigo (2010b); Pham et al. (2011b), the energy balance principle in our particular setting reads as

$$\frac{d}{dt}\mathcal{E}_t(\mathbf{u}_t, \alpha_t, \mathbf{p}_t, \bar{p}_t) = \int_{\partial_D\Omega} \boldsymbol{\sigma}_t\,\mathbf{n} \cdot \dot{\mathbf{U}}_t\, dS - \int_{\partial_F\Omega} \dot{\mathbf{F}}_t \cdot \mathbf{u}_t\, dS. \tag{13}$$

Therefore, (13) is a global (and single) equation which involves the total energy of the whole body and which must hold at every time. Note that the right hand side term in (13) involves the rate of the data whereas the rate $\dot{\boldsymbol{\xi}}_t$ of the state field will appear in the time derivative of the total energy.

2.3.4. Consequences of the principles of irreversibility, stability and energy balance on the evolution law

Using the above three general principles with the particular form of the total energy functional gives a set of necessary conditions that the evolution must satisfy. The details of this construction of the evolution problem are given in the Appendix to which the reader is invited to refer in order to understand the origin of each condition. All these conditions are summarized in Table 2 in the multi-dimensional case. Note that these conditions are necessary but in general not sufficient in order that the "true" stability condition (12) be satisfied at each time of the evolution. One must also verify the so-called second order stability conditions. But these additional conditions will not be used explicitly here and the interested reader can refer to Pham et al. (2011b); Pham and Marigo (2013b); Sicsic et al. (2013) where they play an essential role to select the good evolutions in the cases where many evolutions satisfy the first order stability conditions.

2.4. Constraint on the constitutive functions

Our model (4) contains three state functions: $\mathtt{E}(\alpha)$ (which contains for an isotropic material two scalar state functions, namely $\mathsf{Y}(\alpha)$ and $\nu(\alpha)$ giving the Young modulus and the Poisson ratio), $\mathsf{d}(\alpha)$ and $\bar{\sigma}_{\mathsf{p}}(\alpha)$ which give the dependence of the stiffness, the local damage dissipated energy and the plastic yield stress on the damage variable. The physical meaning of these constitutive functions dictates some natural constraints to be required.

We start from the function $\alpha \mapsto \mathsf{d}(\alpha)$, fixing the amount of dissipated energy with respect to the damage state. Specifically, we assume that it is smooth monotonically increasing function with

$$\mathsf{d}(0) = 0, \qquad \mathsf{d}'(\alpha) > 0,\ \forall \alpha \in [0, 1), \qquad \mathsf{d}(1) = \mathsf{d}_1 < +\infty. \tag{14}$$

name	*statement*	*domain*
stress-strain relation	$\boldsymbol{\sigma} = \mathtt{E}(\alpha)(\nabla_s \mathbf{u} - \mathbf{p})$	Ω
irreversibility	$\dot{\alpha} \geq 0$	Ω
equilibrium in the bulk	$\mathbf{div}\boldsymbol{\sigma} = \mathbf{0}$	$\Omega \setminus J(\boldsymbol{\xi})$
damage criterion in the bulk	$\mathtt{d}'(\alpha) + \sigma_{\mathtt{P}}'(\alpha)\bar{p}^R - \frac{1}{2}\mathtt{C}'(\alpha)\boldsymbol{\sigma}\cdot\boldsymbol{\sigma} - 2\mathtt{d}_1\ell^2\Delta\alpha \geq 0$	$\Omega \setminus J(\boldsymbol{\xi})$
damage consistency in the bulk	$\Big(\mathtt{d}'(\alpha) + \sigma_{\mathtt{P}}'(\alpha)\bar{p}^R - \frac{1}{2}\mathtt{C}'(\alpha)\boldsymbol{\sigma}\cdot\boldsymbol{\sigma} - 2\mathtt{d}_1\ell^2\Delta\alpha\Big)\dot{\alpha} = 0$	$\Omega \setminus J(\boldsymbol{\xi})$
plastic yield criterion in the bulk	$\|\boldsymbol{\sigma}^D\| \leq k_N\, \sigma_{\mathtt{P}}(\alpha)$	$\Omega \setminus J(\boldsymbol{\xi})$
plastic flow rule in the bulk	$\dot{\mathbf{p}}^R = \|\dot{\mathbf{p}}^R\| \dfrac{\boldsymbol{\sigma}^D}{k_N \sigma_{\mathtt{P}}(\alpha)}$	$\Omega \setminus J(\boldsymbol{\xi})$
equilibrium on the jump set	$[\![\boldsymbol{\sigma}]\!]\mathbf{n} = \mathbf{0}$	$J(\boldsymbol{\xi})$
damage criterion on the jump set	$\sigma_{\mathtt{P}}'(\alpha)\bar{P} - 2\mathtt{d}_1\ell^2[\![\partial\alpha/\partial n]\!] \geq 0$	$J(\boldsymbol{\xi})$
damage consistency on the jump set	$\Big(\sigma_{\mathtt{P}}'(\alpha)\bar{P} - 2\mathtt{d}_1\ell^2[\![\partial\alpha/\partial n]\!]\Big)\dot{\alpha} = 0$	$J(\boldsymbol{\xi})$
plastic yield criterion on the jump set	$\|\boldsymbol{\sigma}\mathbf{n} - (\boldsymbol{\sigma}\mathbf{n}\cdot\mathbf{n})\,\mathbf{n}\| \leq \kappa_N \sigma_{\mathtt{P}}(\alpha)$	$J(\boldsymbol{\xi})$
plastic flow rule on the jump set	$[\![\dot{\mathbf{u}}]\!] = \|[\![\dot{\mathbf{u}}]\!]\| \dfrac{\boldsymbol{\sigma}\mathbf{n} - (\boldsymbol{\sigma}\mathbf{n}\cdot\mathbf{n})\,\mathbf{n}}{\kappa_N \sigma_{\mathtt{P}}(\alpha)}$	$J(\boldsymbol{\xi})$
Dirichlet boundary condition	$\mathbf{u} = \mathbf{U}$	$\partial_D\Omega$
Neumann boundary condition	$\boldsymbol{\sigma}\mathbf{n} = \mathbf{F}$	$\partial_F\Omega$
damage boundary condition	$\dfrac{\partial\alpha}{\partial n} \geq 0$	$\partial\Omega$
damage consistency on the boundary	$\dfrac{\partial\alpha}{\partial n}\,\dot{\alpha} = 0$	$\partial\Omega$

Table 2: In the multi-dimensional case, the conditions that the evolution must verify in order that the irreversibility condition, the first order stability conditions and the energy balance are satisfied. Note in particular that the cumulated plastic strain is present in the damage condition and since $\sigma_{\mathtt{P}}' < 0$ the damage critical stress is monotonically decreasing when the plasticity evolves. Note also all the conditions which are obtained on the jump set and which are rarely mentioned in the literature. These latter conditions are essential to obtain the cohesive law as we will see in the next sections.

Concerning the stiffness decrement due to damage, we limit here the attention to the case where

$$\mathtt{E}(\alpha) = \mathtt{a}(\alpha)\,\mathtt{E}_0$$

is given in term of one scalar function $\mathtt{a}(\alpha)$ and the initial sound stiffness $\mathtt{E}_0$. (Of course, more general cases could be considered and that will be the subject of future works.) In isotropic material such an assumption corresponds to the following dependence

$$\mathtt{Y}(\alpha) = \mathtt{a}(\alpha)\,\mathtt{Y}_0, \qquad \nu(\alpha) = \nu_0, \tag{15}$$

for the Young and Poisson moduli respectively. Hence the function $\alpha \mapsto \mathtt{a}(\alpha)$ gives the evolution of the material Young modulus with its damage state. We assume that it is a smooth monotonically decreasing function with

$$\mathtt{a}(0) = 1, \qquad \mathtt{a}'(\alpha) < 0,\ \forall\alpha \in [0,1), \qquad \mathtt{a}(1) = \mathtt{a}'(1) = 0. \tag{16}$$

Additional contraints are needed on the constitutive function $\alpha \mapsto \mathtt{a}(\alpha)$ in order to obtain strain-

hardening and stress-softening behaviors of the material. To this aim, one defines the following sets:

$$\mathcal{D}(\alpha) = \left\{ \boldsymbol{\varepsilon} \in \mathbb{M}_s^N \ | \ -\tfrac{1}{2}\mathbb{E}'(\alpha)\boldsymbol{\varepsilon}\cdot\boldsymbol{\varepsilon} \leq \mathsf{d}'(\alpha) \right\}, \qquad \mathcal{D}^*(\alpha) = \left\{ \boldsymbol{\sigma} \in \mathbb{M}_s^N \ | \ \tfrac{1}{2}\mathbb{C}'(\alpha)\boldsymbol{\sigma}\cdot\boldsymbol{\sigma} \leq \mathsf{d}'(\alpha) \right\}, \tag{17}$$

which represent the domains of elasticity associated with the damage criterion at vanishing cumulated plasticity $\bar{p}$, and

$$\mathcal{P}^*(\alpha) = \left\{ \boldsymbol{\sigma} \in \mathbb{M}_s^N \ | \ \|\boldsymbol{\sigma}^D\| \leq k_N \sigma_{\mathsf{P}}(\alpha) \right\}, \tag{18}$$

which represents the stress domain of elasticity associated with the plasticity criterion. All these elastic domains depend on the damage state. Note that, since $\mathsf{a}(\alpha) = \mathbb{E}_0^{-1}\mathbb{E}(\alpha)$, the inequality defining $\mathcal{D}^*(\alpha)$ can be read as

$$\mathbb{E}_0^{-1}\boldsymbol{\sigma}\cdot\boldsymbol{\sigma} \leq \frac{\sigma_{\mathsf{D}}^2(\alpha)}{\mathsf{Y}_0} := \frac{2\,\mathsf{d}'(\alpha)}{(1/\mathsf{a})'(\alpha)}.$$

The definitions of $\mathcal{D}^*(0)$ and $\mathcal{P}^*(0)$ introduce two thresholds, $\bar{\sigma}_{\mathsf{D}} := \sigma_{\mathsf{D}}(0)$ and $\bar{\sigma}_{\mathsf{P}} := \sigma_{\mathsf{P}}(0)$, for the stress; whether $\bar{\sigma}_{\mathsf{D}} < \bar{\sigma}_{\mathsf{P}}$ or $\bar{\sigma}_{\mathsf{D}} > \bar{\sigma}_{\mathsf{P}}$ discriminates if, in a mono-axial traction test, damage or plasticity will evolve first; thus $\bar{\sigma}_{\mathsf{D}}$ and $\bar{\sigma}_{\mathsf{P}}$ could be interpreted as the initial yield limits.

The strain-hardening property and the stress-softening properties are respectively equivalent to the growth of the set $\mathcal{D}(\alpha)$ and to the decrease of the set $\mathcal{D}^*(\alpha)$ with respect to the damage variable; these requirements translate into the following requests:

$$\text{Strain hardening condition :} \quad \alpha \mapsto \frac{\mathsf{d}'(\alpha)}{|\mathsf{a}'(\alpha)|} \ \text{ is monotonically increasing,} \tag{19}$$

and

$$\text{Stress softening condition :} \quad \alpha \mapsto \frac{\mathsf{d}'(\alpha)}{(1/\mathsf{a})'(\alpha)} \ \text{ is monotonically decreasing.} \tag{20}$$

Finally, it would be natural to require that the plastic yield stress progressively decreases when damage grows and finally vanishes when the material is fully damaged. Within this softening behavior framework, we assume the following properties for the plastic yield stress state function $\alpha \mapsto \sigma_{\mathsf{P}}(\alpha)$:

$$\text{Plastic yield stress softening :} \quad \sigma_{\mathsf{P}}(0) = \bar{\sigma}_{\mathsf{P}} > 0, \quad \sigma_{\mathsf{P}}'(\alpha) < 0, \ \forall \alpha \in [0,1), \quad \sigma_{\mathsf{P}}(1) = 0, \ \sigma_{\mathsf{P}}'(1) \leq 0. \tag{21}$$

Accordingly, our model is quite different of Ambrosio et al. (2012); Del Piero et al. (2012) even if those models have also the goal for coupling fracture with plasticity by using a variational approach.

2.5. A family of admissible constitutive functions

A useful choice of the constitutive function respecting the conditions given above is the following one which depends on three dimensionless parameters $\mathsf{k} > 1$, $\theta > 0$, $\mathsf{n} > 0$ and on three parameters characterizing the material stiffness, the material strength and the material length, namely Y_0, $\bar{\sigma}_{\mathsf{D}}$, ℓ:

$$\mathsf{a}(\alpha) = \frac{1-\mathsf{w}(\alpha)}{1+(\mathsf{k}-1)\mathsf{w}(\alpha)}, \qquad \mathsf{d}(\alpha) = \frac{\mathsf{k}\bar{\sigma}_{\mathsf{D}}^2}{2\mathsf{Y}_0}\mathsf{w}(\alpha), \qquad \sigma_{\mathsf{P}}(\alpha) = (1-\mathsf{w}(\alpha))^{\mathsf{n}}\theta\bar{\sigma}_{\mathsf{D}}, \tag{22}$$

where

$$\mathsf{w}(\alpha) = 1-(1-\alpha)^2. \tag{23}$$

Thus the state functions depend in fact on the variable $\omega = \mathsf{w}(\alpha)$ which grows from 0 to 1 as α does. Accordingly, one gets

$$\sigma_{\mathsf{D}}(\alpha) = (1-\mathsf{w}(\alpha))\bar{\sigma}_{\mathsf{D}} = (1-\alpha)^2\bar{\sigma}_{\mathsf{D}} \tag{24}$$

and

$$\mathsf{d}_1 = \frac{\mathsf{k}\bar{\sigma}_{\mathsf{D}}^2}{2\mathsf{Y}_0}, \qquad \bar{\sigma}_{\mathsf{P}} = \theta\bar{\sigma}_{\mathsf{D}}.$$

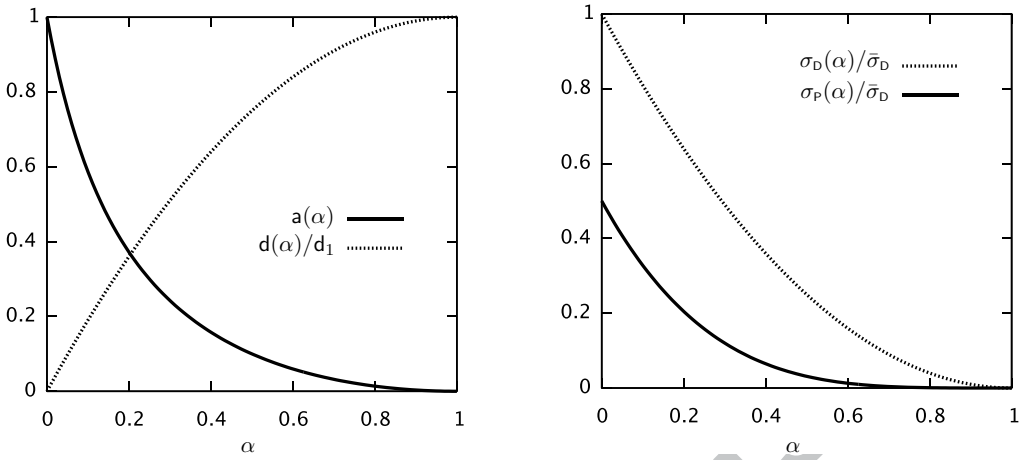

Figure 4: Constitutive functions as in (22)–(24) when $\mathsf{k} = 3$, $\mathsf{n} = 2$ and $\theta = 1/2$.

The solid curves in Figure 4 illustrate the dependences of the constitutive functions on the damage variable for $\mathsf{k} = 3$, $\mathsf{n} = 2$ and $\theta = 1/2$. In Sect. 3 we will discuss in some details the class of models $\mathsf{k} > 1$, $\mathsf{n} \geq 1$ and $\theta < 1$ in which this choice falls; this class physically corresponds to the stress-strain relation shown in Fig. 5, where a purely plastic phase is followed by a coupled evolution of damage and plasticity.

The conditions (14) and (16), the strain hardening condition (19), the softening condition (20) and the plastic yield softening condition (21) are automatically satisfied. The parameter θ represents the ratio between $\bar{\sigma}_{\mathsf{P}}$ and $\bar{\sigma}_{\mathsf{D}}$. The limit case where $\theta = +\infty$ would correspond to a pure damage model without plasticity. It corresponds to the type of damage models which is used in the variational approach to fracture, see Amor et al. (2009); Pham et al. (2011a,b); Sicsic and Marigo (2013), and is close to those used in Lorentz et al. (2011) for quasi-brittle materials.

3. Homogeneous solutions and their stability

Let us study the response predicted by the damage-plasticity coupled model when a single material point is submitted to a uniaxial traction test where $\boldsymbol{\sigma} = \sigma \mathbf{e}_1 \otimes \mathbf{e}_1$ and where the associated strain component $\varepsilon = \varepsilon_{11}$ is controlled. The axial component p_{11} of the plastic strain is denoted p and the cumulated plastic strain is given by $\dot{\bar{p}} = |\dot{p}|$. The state of the material point can be identified with the quadruple $(\varepsilon, \alpha, p, \bar{p})$. We assume that the material point is at time 0 in the unstrained, unstressed and undamaged state, *i.e.* $(\varepsilon_0, \alpha_0, p_0, \bar{p}_0) = (0, 0, 0, 0)$, and then is submitted to an increasing uniaxial stretching where ε grows from 0 to $+\infty$. Accordingly, we can assimilate the time parameter with the strain, *i.e.* $\varepsilon = t$. The problem is to find the evolution of $(\alpha, p, \bar{p})$ with ε. That evolution is assumed to be smooth, in the sense that $\varepsilon \mapsto (\alpha_\varepsilon, p_\varepsilon, \bar{p}_\varepsilon)$ are at least absolutely continuous, and governed by the stress-strain relation, the damage irreversibility condition, the damage and plasticity yield criteria, the damage consistency equation and the plasticity flow rule. For the reader convenience, these equations, derived in the previous section within a three-dimensional

setting, are here reported in scalar form:

$$\begin{aligned}
\text{stress-strain relation} &: \sigma = \mathsf{a}(\alpha)\mathsf{Y}_0(\varepsilon - p), && (25)\\
\text{irreversibility} &: 0 \le \alpha \le 1, \quad \dot\alpha \ge 0, && (26)\\
\text{damage criterion} &: -\tfrac{1}{2}\mathsf{a}'(\alpha)\mathsf{Y}_0(\varepsilon - p)^2 - \mathsf{d}'(\alpha) - \sigma_{\mathsf{P}}'(\alpha)\bar p \le 0 \quad \text{if} \quad \alpha < 1, && (27)\\
\text{plastic yield criterion} &: |\sigma| - \sigma_{\mathsf{P}}(\alpha) \le 0, && (28)\\
\text{damage consistency relation} &: \Big(\tfrac{1}{2}\mathsf{a}'(\alpha)\mathsf{Y}_0(\varepsilon - p)^2 + \mathsf{d}'(\alpha) + \sigma_{\mathsf{P}}'(\alpha)\bar p\Big)\,\dot\alpha = 0, && (29)\\
\text{plastic flow rule} &: \sigma_{\mathsf{P}}(\alpha)\,|\dot p| - \sigma\dot p = 0. && (30)
\end{aligned}$$

Clearly when the strain fields are identified with scalar fields, as done here and in the following section, the request on the plastic strains to be deviatoric must be removed. While the study is trivial in the case of uncoupled models, it becomes much more difficult in the case of a coupling. In particular, the existence of the response is not ensured in the whole range of strains without introducing additional assumptions on the constitutive relations. Moreover, one can obtain a great variety of responses according to the values of the material parameters entering in the model. Thus we limit the analysis to the class of constitutive functions (22) with $\mathsf{k} > 1$, $\mathsf{n} \ge 1$ and $\theta < 1$. This case seems to be particularly relevant for many applications; possible responses in terms of stress-strain relationship are depicted in Fig. 5.

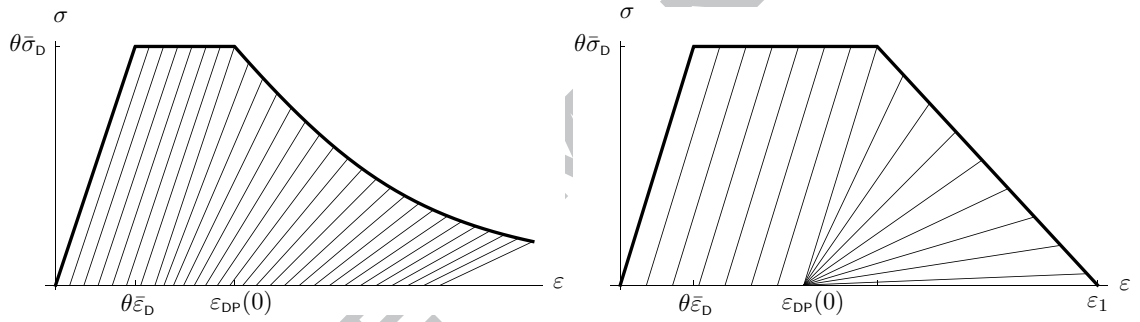

Figure 5: Response of the volume element in the case $\theta < 1$. Left: for $\mathsf{n} > 1$, the response corresponds to the sequence **E**–**P**–**DP**; Right: for $\mathsf{n} = 1$, the response corresponds to the sequence **E**–**P**–**D**–**F**.

Starting from a sound, unstrained and unstressed state, we find first an elastic stage **E**; comparing the two yield functions (27)-(28) at $\alpha = p = \bar p = 0$ we find that the limit strain $\bar\varepsilon_{\mathsf{I}}$ for the elastic stage is

$$\bar\varepsilon_{\mathsf{I}} = \min\{\bar\varepsilon_{\mathsf{D}}, \bar\varepsilon_{\mathsf{P}}\}, \quad \bar\varepsilon_{\mathsf{D}} := \sqrt{\frac{2\mathsf{d}'(0)}{|\mathsf{a}'(0)|\,\mathsf{Y}_0}} = \frac{\bar\sigma_{\mathsf{D}}}{\mathsf{Y}_0}, \quad \bar\varepsilon_{\mathsf{P}} := \frac{\sigma_{\mathsf{P}}(0)}{\mathsf{Y}_0} = \frac{\theta\bar\sigma_{\mathsf{D}}}{\mathsf{Y}_0} = \theta\bar\varepsilon_{\mathsf{D}};$$

Since $\theta < 1$ then $\bar\varepsilon_{\mathsf{I}} \equiv \theta\bar\varepsilon_{\mathsf{D}}$ and the plastic yield is firstly reached. During the elastic stage **E**, we have

$$\forall\varepsilon \in [0, \theta\bar\varepsilon_{\mathsf{D}}], \quad \alpha_\varepsilon = 0, \quad p_\varepsilon = \bar p_\varepsilon = 0, \quad \sigma = \mathsf{Y}_0\,\varepsilon.$$

During the plastic stage **P**, we have

$$\forall\varepsilon \in [\theta\bar\varepsilon_{\mathsf{D}}, \varepsilon_{\mathsf{DP}}(0)], \quad \alpha_\varepsilon = 0, \quad p_\varepsilon = \bar p_\varepsilon = \varepsilon - \theta\bar\varepsilon_{\mathsf{D}}, \quad \sigma = \theta\bar\sigma_{\mathsf{D}}.$$

The plastic stage ends at the limit strain $\varepsilon_{\mathsf{DP}}(0)$. Indeed, during the plastic stage, the plastic strain accumulation reduces the damage yield limit until the current value of stress is reached. Hence one seeks for the value of strain where both yield criteria are satisfied: eliminating the plastic strain leads to the following

$$\varepsilon_{\mathsf{DP}}(\alpha) = \Big((1-\alpha)^{-2\mathsf{n}+2}\mathsf{k} - \theta^2(1-\alpha)^{2\mathsf{n}-2}\Big(\mathsf{k} - 2\mathsf{n}\big(1 + (\mathsf{k}-1)(2-\alpha)\alpha\big)\Big)\Big)\frac{\bar\varepsilon_{\mathsf{D}}}{2\theta\mathsf{n}}.$$

As in the plastic stage **P** we had $\alpha = 0$, we immediately get:

$$\varepsilon_{\mathsf{DP}}(0) = \theta\bar{\varepsilon}_{\mathsf{D}} + \frac{\mathsf{k}(1-\theta^2)}{2\mathsf{n}\theta}\bar{\varepsilon}_{\mathsf{D}};$$

a value strictly larger than $\theta\bar{\varepsilon}_{\mathsf{D}}$, see Fig. 5. Finally, as for $\varepsilon = \varepsilon_{\mathsf{DP}}(0)$ the damage yield has been reached, the damage evolves. It turns out that, for this class of constitutive parameters, both the yield limits are identically satisfied; hence we have a damage-plastic stage **DP**, where both damage and plasticity could evolve. Specifically we have

$$\forall \varepsilon \in [\varepsilon_{\mathsf{DP}}(0), \varepsilon_{\mathsf{DP}}(\alpha \to 1)], \quad \alpha_\varepsilon = \varepsilon_{\mathsf{DP}}^{-1}(\varepsilon), \quad p_\varepsilon = \bar{p}_\varepsilon = \pi_{\mathsf{DP}}(\alpha_\varepsilon), \quad \sigma = \sigma_{\mathsf{P}}(\alpha_\varepsilon),$$

where

$$\pi_{\mathsf{DP}}(\alpha) := \frac{\mathsf{k}\bar{\varepsilon}_{\mathsf{D}}}{2\theta\mathsf{n}}\Big((1-\alpha)^{-2\mathsf{n}+2} - \theta^2(1-\alpha)^{2\mathsf{n}-2}\Big).$$

Note that for $\mathsf{n} > 1$ the **DP** stage continues up to infinity as $\varepsilon_{\mathsf{DP}}(\alpha \to 1) = +\infty$ and the plasticity actually increases monotonically (Fig. 5 left). However, when $\mathsf{n} = 1$, we have

$$\varepsilon_{\mathsf{DP}}(1) = \frac{\mathsf{k}(1+\theta^2)\bar{\varepsilon}_{\mathsf{D}}}{2\theta} =: \varepsilon_1, \qquad p_\varepsilon = \bar{p}_\varepsilon = \frac{\mathsf{k}(1-\theta^2)}{2\theta}\bar{\varepsilon}_{\mathsf{D}}.$$

Thus for $\mathsf{n} = 1$ the plastic strain remains fixed at the value reached at the end of the plastic stage **P**, and we actually have a pure damage stage **D**, see Fig.5 (right). A totally damaged material **F**, namely the condition $\alpha = 1$, is reached for a finite strain as $\varepsilon_1 < \infty$.

4. Closed form solution for the one-dimensional traction test

4.1. General assumptions

Again with the purpose of simulating a uniaxial traction test, we now allow the fields to be functions of one spatial coordinate. To this aim we consider $\Omega = (0, L)$ as the reference configuration of a one-dimensional body called *the bar*. Its end $x = 0$ is fixed and the end $x = L$ is submitted to a time dependent displacement U_t with $U_0 = 0$. The bar is made of a material whose local behavior is given by the plasticity-damage models described in the previous section. The equations governing the evolution of the bar with time t are the scalar form of the equations derived in Sect. 2; their solution is given is the map $t \mapsto (u_t, \alpha_t, p_t, \bar{p}_t)$ for $t \geq 0$, where u_t, α_t, p_t and $\bar{p}_t$ denote now, respectively, the displacement field, the damage field, the plastic strain field and the cumulated plastic strain field of the bar at time t. We assume that, at time $t = 0$, the bar is sound and was never plasticized so that $\alpha_0 = p_0 = \bar{p}_0 = 0$ everywhere in Ω.

It is easy to check that the homogeneous response, *i.e.* the response such that $u_t(x) = U_t x/L$, $\alpha_t(x) = \alpha_t$ and $p_t(x) = p_t$ for all $x \in \Omega$, is still possible. In the case where $U_t = tL$, *i.e.* for a monotonically increasing traction test, the homogeneous response is precisely that obtained in the previous section for the volume element. This evolution, namely the **E**, **P**, and **DP** stages described above, satisfies the irreversibility condition, the first order stability conditions and the energy balance because, in particular, the gradient of damage vanishes and $J(\boldsymbol{\xi}_t) = \emptyset$. However, we are no more ensured that it is the unique solution. Moreover, we are not ensured that the local stability condition (12) is satisfied by the homogeneous response. If we refer to what happens in the case of gradient damage models with softening (without plasticity), we know that the homogeneous response is unique and stable if and only if the length L of the bar is sufficiently small by comparison with the internal length ℓ of the material Pham et al. (2011b); Pham and Marigo (2013b). When the length of the bar is large enough, the homogeneous response is not stable and it is possible to construct non homogeneous responses. Accordingly, we propose here to follow the same procedure and, assuming that L is sufficiently large by comparison with ℓ, to construct a response where the damage, when it appears, remains localized on a time-dependent part of the bar. To construct such an evolution, we follow the method proposed in Pham et al. (2011b); Pham and Marigo (2013a).

To simplify the presentation and to prevent from considering too many cases, we construct such non homogeneous responses for the family of models considered at Section 2.5 only. Therefore, a, d and σ_{P} are given by (22)-(23) with $\mathsf{k} > 1$, $\mathsf{n} = 1$ and $\theta < 1$. Despite the cases $\mathsf{n} > 1$ could be treated similarly, we focus the attention on the case $\mathsf{n} = 1$ because the solution can be obtained in a closed form and all the steps for constructing the solution are easier.

4.2. Plasticity stage followed by damage localization with nucleation and growth of a cohesive crack

The analysis starts at a time when the damage yield criterion is reached somewhere in the bar. This time t_c corresponds to the end a $\mathbf{P}$ stage as $\theta < 1$. We will assume, to simplify the presentation, that the plastic strain field and the cumulated plastic strain field are uniform at t_c. Hence, the state of the bar at t_c is $\boldsymbol{\xi}_{t_c} = (\varepsilon_{\mathsf{DP}}(0)x, 0, \pi_{\mathsf{DP}}(0), \pi_{\mathsf{DP}}(0))$, the stress is $\sigma_{t_c} = \theta\bar{\sigma}_{\mathsf{D}}$ and the damage yield criterion is also reached at every point of the bar:

$$\alpha(x) = 0, \quad p(x) = \bar{p}(x) = \pi_{\mathsf{DP}}(0) = \frac{(1-\theta^2)\mathsf{k}\bar{\varepsilon}_{\mathsf{D}}}{2\theta}, \quad \sigma = \theta\bar{\sigma}_{\mathsf{D}}.$$

When $t > t_c$, we assume that σ_t is monotonically decreasing from σ_{t_c} to 0. We seek for non homogeneous evolutions such that the damage zone is the interval $(x_1 - \Delta_t, x_1 + \Delta_t)$ where x_1 is an arbitrary point of the bar sufficiently far from its ends so that $0 < x_1 - \Delta_t \leq x_1 + \Delta_t < L$. Thus, we exclude the case where the damage zone is at the boundary. The half width Δ_t of the damage zone, which can depend on time, has to be determined. We will assume that the center x_1 of the damage zone is the unique possible singular point, *i.e.* $J(\boldsymbol{\xi}_t) = \emptyset$ or $J(\boldsymbol{\xi}_t) = \{x_1\}$.

Therefore, the plasticity can only evolve at x_1 by virtue of (43) and remains equal to $\pi_{\mathsf{DP}}(0)$ otherwise,

$$p_t^R(x) = \bar{p}_t^R(x) = \pi_{\mathsf{DP}}(0), \quad \forall x \in (0, L) \setminus \{x_1\}, \quad \forall t \geq t_c.$$

Accordingly, by virtue of (53), the damage field must satisfy when $0 < \sigma < \theta\bar{\sigma}_{\mathsf{D}}$:

$$-\mathsf{C}'(\alpha)\sigma^2 + 2\mathsf{d}'(\alpha) + 2\sigma_{\mathsf{P}}'(\alpha)\pi_{\mathsf{DP}}(0) - 4\mathsf{d}_1\ell^2\alpha'' = 0 \quad \text{in} \quad I_\sigma \setminus \{x_1\}, \tag{31}$$

and

$$\alpha(x_1 \pm \Delta_\sigma) = \alpha'(x_1 \pm \Delta_\sigma) = 0, \tag{32}$$

where $\mathsf{C}(\alpha) = 1/(\mathsf{a}(\alpha)\mathsf{Y}_0)$ is the compliance state function, $I_\sigma = (x_1 - \Delta_\sigma, x_1 + \Delta_\sigma)$ denotes the damage zone and Δ_σ is its half-width which has to be determined. The conditions at x_1 depends on whether x_1 is singular or not, but in any case and since $\mathsf{n} = 1$ the plasticity criterion requires that

$$\sigma \leq \sigma_{\mathsf{P}}(\alpha(x_1)) = \theta(1 - \alpha(x_1))^2\bar{\sigma}_{\mathsf{D}}. \tag{33}$$

Multiplying (31) by $2\alpha'$, one obtains a first integral with the constant given by (32). Specifically, one gets

$$2\mathsf{d}_1\ell^2\alpha'^2 = 2\mathsf{d}(\alpha) - 2(\sigma_{\mathsf{P}}(0) - \sigma_{\mathsf{P}}(\alpha))\pi_{\mathsf{DP}}(0) - (\mathsf{C}(\alpha) - \mathsf{C}(0))\sigma^2 \quad \text{in} \quad I_\sigma \setminus \{x_1\}. \tag{34}$$

This property holds for any plasticity-damage model. In the case of the models given by (22)-(23) with $\mathsf{n} = 1$, after introducing the variable ω, the first integral eventually reads as

$$\ell^2\omega'^2 = 4\theta^2\omega(\bar{\omega}_\sigma - \omega) \quad \text{where} \quad \bar{\omega}_\sigma = 1 - \frac{\sigma^2}{\theta^2\bar{\sigma}_{\mathsf{D}}^2}.$$

Hence, in the normalized phase plane $(\omega, \ell\omega'/2\theta)$, the first integral is a circle of center $\bar{\omega}_\sigma/2$ and radius $\bar{\omega}_\sigma/2$. The plasticity criterion (33) requires that

$$\omega(x_1) \leq \omega_\sigma^* := 1 - \frac{\sigma}{\theta\bar{\sigma}_{\mathsf{D}}}.$$

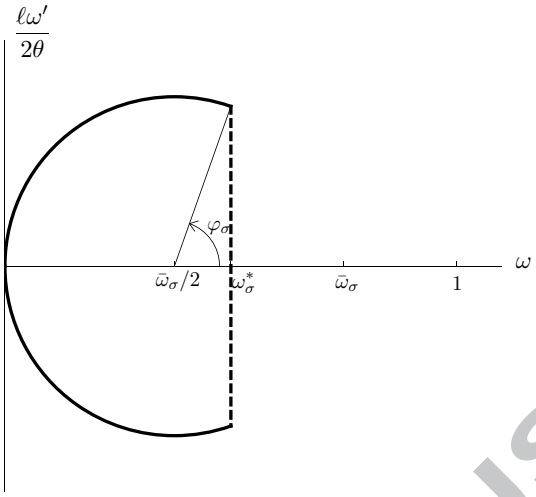

Figure 6: In the case $\theta < 1$ and $\mathsf{n} = 1$, construction of the solution in the phase plane at a given stress $\sigma < \theta\bar\sigma_{\mathrm{D}}$. The circle represents the damage field and the dashed line corresponds to the jump of ω' at the center of the damage zone.

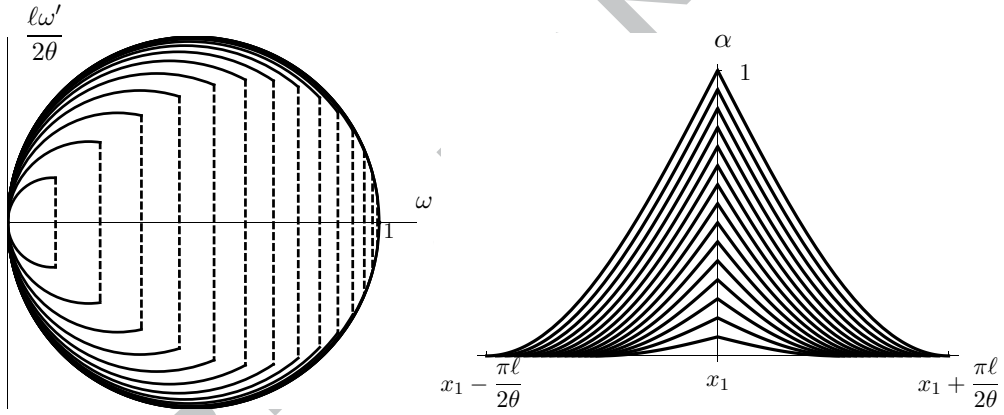

Figure 7: Case with $\theta = 2/3$, $\mathsf{n} = 1$ and $\mathsf{k} = 4$: evolution of the damage after the plasticity stage. On the left, evolution in the phase plane $(\omega, \ell\omega'/2\theta)$; on the right, evolution in the physical space. The presence of a cohesive crack from the beginning of the damage process is visible on both spaces.

But since $\omega^*_\sigma < \bar\omega_\sigma$ as soon as $\sigma < \theta\bar\sigma_{\mathrm{D}}$, ω' is necessarily discontinuous at x_1 and hence x_1 is a singular point, see Figure 6. Therefore, a cohesive crack appears as soon as $\sigma < \theta\bar\sigma_{\mathrm{D}}$ and, by virtue of (54) and(58), one must have

$$\omega(x_1) = \omega^*_\sigma, \qquad \sigma'_{\mathrm{p}}(\alpha^*_\sigma)[\![u]\!](x_1) = 2\mathsf{d}_1\ell^2[\![\alpha']\!](x_1).$$

Setting $\omega(x) = \bar\omega_\sigma \cos^2\frac{\varphi(x)}{2}$ gives $\ell^2\varphi'^2 = 4\theta^2$. Therefore, the half width Δ_σ of the damage zone is given by

$$\Delta_\sigma = (\pi - \varphi_\sigma)\frac{\ell}{2\theta} \qquad \text{with} \qquad \varphi_\sigma = \arccos\frac{\theta\bar\sigma_{\mathrm{D}} - \sigma}{\theta\bar\sigma_{\mathrm{D}} + \sigma}.$$

So Δ_σ increases from $\pi\ell/4\theta$ to $\pi\ell/2\theta$ when σ goes from $\theta\bar\sigma_{\mathrm{D}}$ to 0. For a given σ, the damage profile in the damage zone is given by

$$\alpha(x) = 1 - \sqrt{1 - \omega(x)} = 1 - \sqrt{1 - \bar\omega_\sigma \cos^2\left(\frac{\varphi_\sigma}{2} + \frac{\theta\,|x - x_1|}{\ell}\right)} \quad \text{in} \quad I_\sigma.$$

Since $\bar{\omega}_\sigma$ is increasing and φ_σ is decreasing (when σ decreases), the damage grows at given x and hence the irreversibility condition is satisfied. The damage evolution is represented on Figure 7 for $\theta = 2/3$.

As long as the cohesive law is concerned, one gets

$$[\![u]\!] = \mathsf{k}\bar{\varepsilon}_{\mathsf{D}}\ell\left(\sqrt{\frac{\theta\bar{\sigma}_{\mathsf{D}}}{\sigma}} - \sqrt{\frac{\sigma}{\theta\bar{\sigma}_{\mathsf{D}}}}\right) \quad \text{or equivalently} \quad \sigma = \theta\sigma_{\mathsf{D}}\left(\sqrt{1+\frac{[\![u]\!]^2}{4\mathsf{k}^2\bar{\varepsilon}_{\mathsf{D}}^2\ell^2}} - \frac{[\![u]\!]}{2\mathsf{k}\bar{\varepsilon}_{\mathsf{D}}\ell}\right)^2 \tag{35}$$

the cohesive crack appearing as soon as the damage starts.

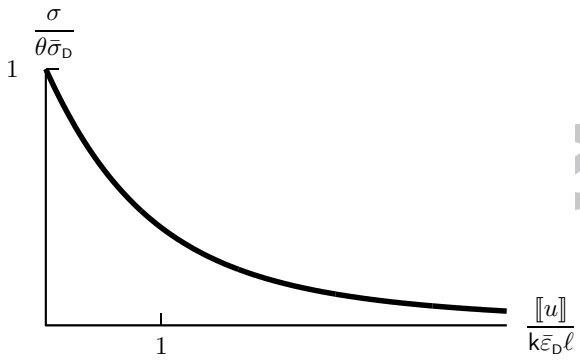

Figure 8: Graph of the cohesive law obtained for $\mathsf{n} = 1$ which gives σ in term of $[\![u]\!]$. Note that the curve is monotonically decreasing, but tends only asymptotically to 0.

When $\sigma = 0$, then $\varphi_0 = 0$, $\bar{\omega}_0 = 1$ and $\alpha(x_1) = 1$. A true crack has nucleated at x_1 and the damage profile is

$$\alpha(x) = 1 - \sin\left(\frac{\theta\,|x-x_1|}{\ell}\right) \text{ in } \left(x_1 - \frac{\pi\ell}{2\theta}, x_1 + \frac{\pi\ell}{2\theta}\right), \qquad \text{when} \quad \sigma = 0. \tag{36}$$

The dissipated energy inside the damage zone at the end of the damage localization process, *i.e.* when $\sigma = 0$ is given by

$$\mathcal{D}_0 = \int_{x_1-\Delta_0}^{x_1+\Delta_0} \left(\mathsf{d}(\alpha(x)) + \sigma_{\mathsf{P}}(\alpha(x))\pi_{\mathsf{DP}}(0) + \mathsf{d}_1\ell^2\alpha'(x)^2\right) dx$$

with α given by (36). A part, namely $2\sigma_{\mathsf{P}}(0)\pi_{\mathsf{DP}}(0)\Delta_0$, was dissipated during the **P** stage. So, if we define $\mathsf{G_c}$ as the dissipated energy due to the damage process alone, then we obtain

$$\mathsf{G_c} := \int_{x_1-\Delta_0}^{x_1+\Delta_0} \left(\mathsf{d}(\alpha(x)) + (\sigma_{\mathsf{P}}(\alpha(x)) - \sigma_{\mathsf{P}}(0))\pi_{\mathsf{DP}}(0) + \mathsf{d}_1\ell^2\alpha'(x)^2\right) dx.$$

After some calculations, one gets

$$\mathsf{G_c} = \frac{\pi\mathsf{k}}{2}\frac{\theta\bar{\sigma}_{\mathsf{D}}^2}{\mathsf{Y}_0}\ell.$$

Note that this value of $\mathsf{G_c}$ involves all the parameters of the model.

5. Numerical implementation

The numerical implementation of the proposed model takes advantage from the variational formulation. Indeed, the stability condition is directly translated into a numerical strategy based on seeking local energy minimizers. The numeric simulations will cover the most delicate aspect of the problem, that is the ability

of the algorithm to understand and describe the plastic localization and the cohesive response in both a one-dimensional and a two-dimensional traction test.

For technical reasons, the constitutive functions used in the numerical simulations are chosen to be:

$$\mathsf{a}(\alpha) = (1-\alpha)^2, \qquad \mathsf{d}(\alpha) = \frac{\bar{\sigma}_{\mathsf{P}}^2}{\theta^2 \mathsf{Y}_0}\alpha, \qquad \sigma_{\mathsf{P}}(\alpha) = (1-\alpha)^2 \bar{\sigma}_{\mathsf{P}} \tag{37}$$

with $0 < \theta < 1$. This model satisfies all the required properties of strain hardening (19), stress softening (20) and plastic yield stress softening (21), but it does not belong to the family of models (22) because of the linear dependence of d on α. However this choice allows to use dedicated libraries for the minimization of the damage variable, which turns out to be a constrained quadratic optimization problem. The material characteristic length ℓ is chosen sufficiently small by comparison to the size L of the body so that damage localization be possible. We still have

$$\bar{\sigma}_{\mathsf{D}} = \frac{\bar{\sigma}_{\mathsf{P}}}{\theta}, \quad \bar{\varepsilon}_{\mathsf{P}} = \frac{\bar{\sigma}_{\mathsf{P}}}{\mathsf{Y}_0}, \quad \bar{\varepsilon}_{\mathsf{D}} = \frac{\bar{\sigma}_{\mathsf{D}}}{\mathsf{Y}_0} = \frac{\bar{\varepsilon}_{\mathsf{P}}}{\theta}$$

and the damage criterion reads now

$$1 - 2(1-\alpha)\theta^2 \frac{\bar{p}}{\bar{\varepsilon}_{\mathsf{P}}} - \frac{\theta^2}{(1-\alpha)^3}\left((1+\nu)\frac{\boldsymbol{\sigma}\cdot\boldsymbol{\sigma}}{\bar{\sigma}_{\mathsf{P}}^2} - \nu\frac{(\mathrm{Tr}\,\boldsymbol{\sigma})^2}{\bar{\sigma}_{\mathsf{P}}^2}\right) - 2\ell^2\Delta\alpha \geq 0.$$

5.1. Time and space discretisation and numeric algorithm

As the imposed displacement boundary conditions will be chosen proportionally to t, the time can be interpreted as a multiplier of the applied external action. We follow the minimizers of the total energy as t is increased in steps of uniform amplitudes until $t = T$ for T sufficiently large.

For both 1D and 2D cases, the code has been implemented within the finite element framework *FEniCS* (Logg et al., 2012). Specifically the displacement and damage fields are projected over a piecewise affine finite element space (1-Lagrange elements) using the same triangulation domain. Motivations for not using higher degree finite elements can be found for example in Bourdin et al. (2000). Conversely, the plastic strain field $\mathbf{p}$ is projected over a discrete discontinuous space (Quadrature elements) defined only over the Gauss integration points. These last correspond to the centers of the elements, as suggested by the local character of the plastic model.

It is worthnoting that apparently there was no chance to describe displacement jumps and plastic singularities leading to a cohesive response since the chosen finite element spaces do not own the capability to describe such solution. Nevertheless and quite surprisingly this kind of response is picked up from the simulations. The reason lies on how plasticity is implemented. Although plasticity is defined over discrete points the contribution of any point is spread over the entire finite element of size h. That is, the numerical approximation has the effect to regularize the displacement and plastic field while the mesh size h plays the role of a convergence parameter. In the following the responses are compared for meshes of different size.

As the energy functional is separately convex in each variable, it seems reasonable to adopt an alternate minimization algorithm respectively in the variables $\mathbf{u}$, $\mathbf{p}$ and α. Hence at a given time step the solution is simply found iterating alternatively on the three following subproblems until convergence:

- the minimization of $\mathcal{E}$ with respect to $\mathbf{u}$ at fixed $\mathbf{p}$ and α: this is a straightforward unconstrained optimization problem solved as an elastic problem with prescribed boundary conditions;
- the minimization of $\mathcal{E}$ with respect to $\mathbf{p}$ at fixed $\mathbf{u}$ and α: this is a nonlinear constrained problem. Since no space derivatives involves the field p the optimality condition is local although non linear. A common solution procedure involves a standard return mapping algorithm;
- the minimization of $\mathcal{E}$ with respect to α at fixed $\mathbf{u}$ and $\mathbf{p}$: this is a box constrained quadratic optimization problem, which can be solved by a linear bound constraint solver; in particular we use the TAO (Toolkit for Advanced Optimization) library[1].

[1] http://www.mcs.anl.gov/research/projects/tao/

5.2. One-dimensional traction test

For the one-dimensional traction test, namely the same problem analytically solved in Sect. 4, we have

$$\Omega = (0,\, L), \qquad u(0) = 0, \quad u(L) = U \text{ with } U \text{ increasing from } 0$$

and the response essentially depends on the two dimensionless parameters ℓ/L and θ. The computations are made with

$$\ell/L = 0.15\sqrt{2} \approx 0.21, \quad \theta = 1/\sqrt{2} \approx 0.71.$$

Following the method described in the previous section, a solution with a damage localization zone can be obtained in a closed form. Let us recall its main features. The elastic stage **E** ends when $U = \bar{\varepsilon}_{\mathsf{P}} L$, then a plastic stage **P** starts during which the plastic strain field remains uniform in space. The plastic stage ends when the damage criterion is reached (everywhere) in the bar. That corresponds to the moment when $U = U_c$ and $p = \bar{p} = p_c$, U_c and p_c being given here by

$$U_c = \varepsilon_{\mathsf{DP}}(0) L := \frac{1+\theta^2}{2\theta^2} \bar{\varepsilon}_{\mathsf{P}} L = 1.5\, \bar{\varepsilon}_{\mathsf{P}} L, \qquad p_c = \pi_{\mathsf{DP}}(0) := \frac{1-\theta^2}{2\theta^2} \bar{\varepsilon}_{\mathsf{P}} = 0.5\, \bar{\varepsilon}_{\mathsf{P}}.$$

For $U > U_c$ damage occurs and the damage field is localized in an interval $I = (x_1 - \Delta, x_1 + \Delta)$, the position of its center x_1 being arbitrary. In the damage zone deprived of its center, *i.e.* in $I \setminus \{x_1\}$, the damage field is given by the first integral (34) which reads here

$$\ell^2 \alpha'(x)^2 = \alpha(x) + \frac{\theta^2 \sigma^2}{2\bar{\sigma}_{\mathsf{P}}^2} \left(\frac{1}{(1-\alpha(x))^2} - 1 \right) - \frac{1-\theta^2}{2} \Big(1 - (1-\alpha(x))^2 \Big).$$

This first integral gives also the width Δ of the damage zone which depends only on σ. At the center x_1, α' and u are discontinuous, a cohesive crack appears and the cohesive law relating $[\![u]\!]$ to σ is obtained by using the plastic yield criterion and the first integral above. Specifically, one gets

$$1 - \alpha(x_1) = \sqrt{\frac{\sigma}{\bar{\sigma}_{\mathsf{P}}}}, \qquad [\![u]\!](x_1) = \frac{2\ell \bar{\varepsilon}_{\mathsf{D}}}{\theta^2} \sqrt{\frac{\bar{\sigma}_{\mathsf{P}}}{\sigma}} \left(\frac{1+\theta^2}{2} + \sqrt{\frac{\sigma}{\bar{\sigma}_{\mathsf{P}}}} + \frac{\sigma}{2\bar{\sigma}_{\mathsf{P}}} - \frac{\theta^2 \sigma^2}{2\bar{\sigma}_{\mathsf{P}}^2} \right).$$

Finally, the stress-displacement relation σ-U is obtained by using the stress-strain relation, the boundary condition and the first integral of the damage criterion,

$$U = [\![u]\!](x_1) + \frac{\sigma}{\mathsf{Y}_0} \int_0^L \frac{dx}{(1-\alpha(x))^2}.$$

Note that the graph σ-U presents a snap-back at U_c when the ratio ℓ/L is small enough. Therefore, if one prescribes a monotonic increasing displacement U, then the evolution is necessarily discontinuous at U_c and the stress jumps from $\bar{\sigma}_{\mathsf{P}}$ to a smaller value which depends on L.

In Figure 9 the analytic solution is compared to the Finite Element approximation with different mesh sizes: 20, 50, 100 and 200 elements in Ω. Thick solid lines are used to plot the analytic response, while dotted, dotted-dashed, dashed and thin solid lines are used to represent the numerical responses at decreasing mesh size. In Fig. 9c and 9d the integral of the cumulated plasticity and stress are plotted against the applied end-displacement U: it is evident the critical value where a displacement jump occurs and the final cohesive phase where despite the existence of $[\![u]\!]$ still the bar sustains a non-vanishing stress σ; the analytic curve is actually the plot of cohesive law (35). For U within the final cohesive phase, we compare the responses in terms of damage $\alpha(x)$ and plastic strain $p(x)$ profiles in Figs. 9a and 9b respectively.

In all these cases, the numeric solutions monotonically converge towards the analytic solution as the mesh size decreases. In particular, comparing Fig. 9b and 9c, one can appreciate a rather surprising mesh independence of the plastic localization. Indeed, for a sequence of decreasing mesh sizes, the numerical approximation mimics the singular part of the plastic response (as discussed before a Dirac delta in $x = x_1$) by a sequence of increasingly localized profiles with monotonically converging subtended areas.

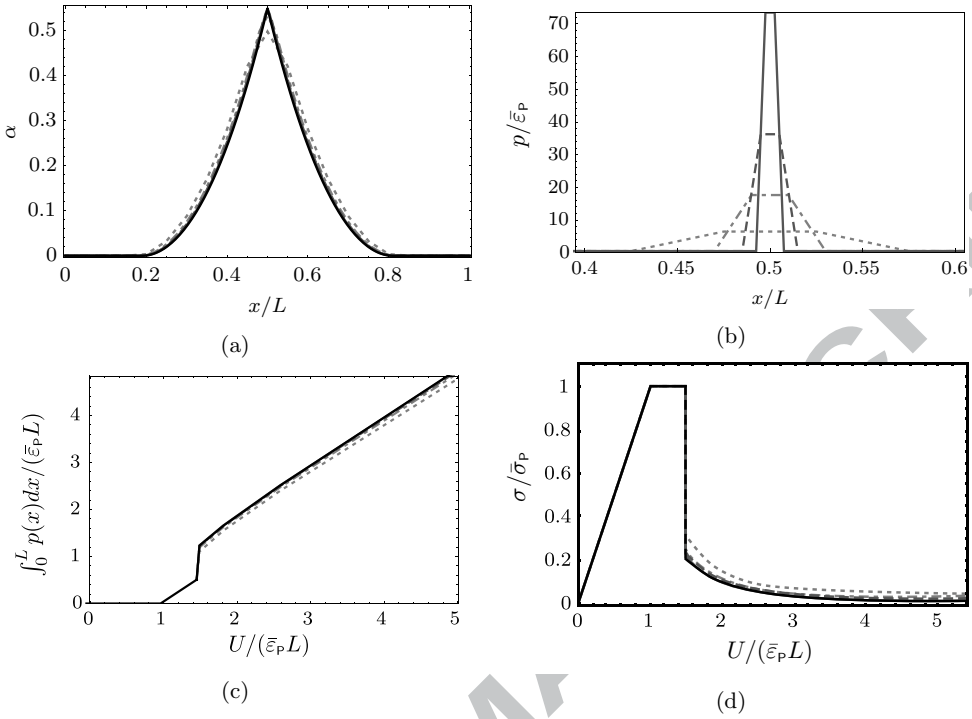

Figure 9: In 1D comparison of the analytic solution (solid black) with the numeric solutions for the different mesh sizes (20 elem. (dotted); 50 elem. (dot-dashed), 100 elem. (dashed), 200 elem. (thin)): (a) and (b) represent respectively the damage field α and the additional plastic strain field $p - p_e$ at a given time step after the occurrence of the cohesive crack; (c) and (d) represent respectively the accumulated plastic strain integrated over the domain and the stress-displacement response.

5.3. Two-dimensional traction test

This simulation has the purpose to highlight the effectiveness of both the model and the numeric implementation in spatial dimensions higher than 1. We choose:

$$\Omega = (0,\, L) \times (0, H), \qquad u_1(x = 0) = 0, \quad u_1(x = L) = U \text{ with } U \text{ increasing from } 0,$$

where $(\mathbf{e}_1,\, \mathbf{e}_2)$ is the natural orthonormal base and the transversal contraction is left free, see Fig. 10a.

Plane strain conditions are assumed and the data are $\ell/L = 0.15\sqrt{2}$, $H/L = 0.2$, $\nu = 0.3$, $\theta = 1/\sqrt{3}$. Accordingly, the deformation remains homogeneous in space during the elastic stage and the plastic stage. The elastic stage ends when $U = U_e$ and $\sigma_{11} = \sigma_e$ with

$$\frac{U_e}{\bar{\varepsilon}_{\text{P}} L} = \frac{1 - \nu^2}{\sqrt{1 - \nu + \nu^2}} \approx 1.024, \qquad \frac{\sigma_e}{\bar{\sigma}_{\text{P}}} = \frac{1}{\sqrt{1 - \nu + \nu^2}} \approx 1.125.$$

The plastic stage ends when the damage criterion is reached everywhere in the specimen. At this moment, the values U_c, σ_{11}^c and $\bar{p}_c$ of the displacement, the normal stress component and the cumulated plastic strain can be obtained in a closed form, but we give here their numerical values only

$$U_c \approx 1.834\ \bar{\varepsilon}_{\text{P}} L, \quad \sigma_{11}^c \approx 1.149\ \bar{\sigma}_{\text{P}}, \quad \bar{p}_c \approx 0.889\ \bar{\varepsilon}_{\text{P}}.$$

All these theoretical values are well captured by the alternate minimization algorithm, see Fig. 10d. After this critical time, the solution can no more be obtained in a closed form and we will refer to the numerical results only. The numerical computations show that, as in the 1D case, the damage localizes in a strip whose width is of the order of the internal length ℓ and a cohesive crack nucleates at its center. The phenomenon

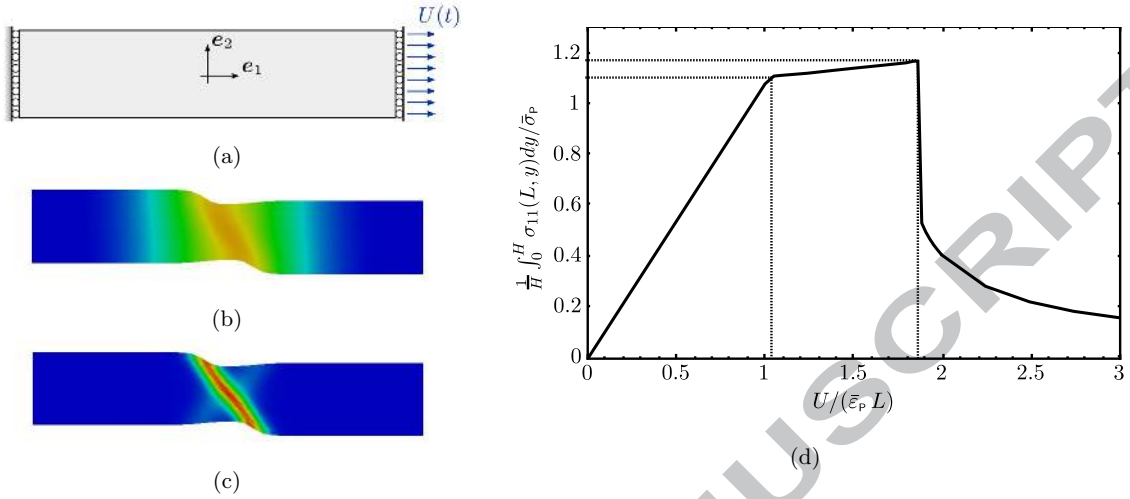

Figure 10: Numerical results for the 2D traction test:
(a) The reference configuration; (b) The damage field plotted on the deformed shape when $U = 2\bar{\varepsilon}_P L$ (blue, $\alpha = 0$; red, $\alpha = 1$); (c) The accumulated plastic strain field plotted on the deformed shape when $U = 2\bar{\varepsilon}_P L$ (blue, $\bar{p} = \min$; red, $\bar{p} = \max$); (d) The average normal stress at $x_1 = L$ versus the average prescribed stretching.

is still brutal in the sense that the evolution is discontinuous at this time and the stress drops. Specifically, in Figure 10d the global response of the specimen is reported; namely the stress component σ_{11}, averaged on the boundary $x = L$, is plotted against the end displacement U. One can see the sudden drop of the stress value when $U \approx 1.7\,\bar{\varepsilon}_P L$ which is accompanied by the formation of a localized plastic field (actually a shear band) in the center of the specimen. For a greater value of the end displacement U, we have plotted in Figs. 10b and 10c the damage field α and the cumulated plastic strain field $\bar{p}$ respectively. As to be expected, the plastic localization describes a shear band which is inclined with respect the axis of traction (the inclination can depend on the width H of the specimen); this zone is centered within the support of the damage profile. However, whilst the size of the damaged zone can be constitutively controlled, being proportional to the internal characteristic length ℓ, the size of the plastic strain localization is inessential and dictated by the mesh size. As in Fig. 9b, it is the actual subtended area in the direction normal to the discontinuity to have a true physical meaning.

6. Perspectives

Let us finish now by some perspectives.

1. We have only considered in the present paper the case where the plasticity criterion is Von Mises criterion. A first natural extension will consist in generalizing our approach to arbitrary convex set.
2. We have chosen here a form of the total energy which is the simplest one to couple damage with plasticity. More complex coupling based on phenomenological considerations or physical mechanisms should deserve to be analyzed.
3. Our approach leads to a competition between the damage criterion and the plastic yield criterion. The latter is unbounded in the direction of hydrostatic pressure while the former one is bounded in every stress direction. Assuming that $\bar{\sigma}_P < \bar{\sigma}_D$, the plastic criterion is reached before the damage criterion in the uniaxial traction problem and consequently the fracture occurs along a shear band where the plasticity is concentrated and which forces the jump discontinuity of the displacement to be tangential.

In more complex situations, it could happen that the damage criterion be reached at a point without any preliminary plasticization (because of a triaxiality effect) and hence that a non cohesive crack nucleates at this point as in the quasi-brittle case. The highlighting of such phenomena will be the goal of future works.

4. Accordingly, the numerical method will be tested on more complex geometry and loading.

A. Construction of the evolution problem from the irreversibility condition, the stability principle and the energy balance

A.1. The first order stability conditions

Dividing (12) by h and passing to the limit when $h \to 0$ yields *the first order stability conditions*:

$$\frac{d}{dh}\mathcal{E}_t\Big(\mathbf{u}_t + h\mathbf{v}, \alpha_t + h\beta, \mathbf{p}_t + h\mathbf{q}, \bar{p}_t + hk_N\|\mathbf{q}\|\Big)\Big|_{h=0} \geq 0, \quad \forall(\mathbf{v}, \beta, \mathbf{q}) \text{ admissible.}$$

Using the definition (9) of the energy and the assumed forms of the field leads to

$$\begin{aligned} 0 \;\leq\; & \int_{\Omega\setminus(J(\boldsymbol{\xi}_t)\cup J(\mathbf{v}))} \boldsymbol{\sigma}_t \cdot (\nabla_s \mathbf{v} - \mathbf{q}^R)\, d\mathbf{x} + \int_{\Omega\setminus J(\mathbf{v})} \sigma_{\mathsf{P}}(\alpha_t) k_N \|\mathbf{q}^R\|\, d\mathbf{x} + \int_{J(\mathbf{v})} \sigma_{\mathsf{P}}(\alpha_t)\kappa_N \|[\![\mathbf{v}]\!]\|\, dS \\ + & \int_\Omega \Big(\mathsf{d}'(\alpha_t) - \tfrac{1}{2}\mathsf{C}'(\alpha_t)\boldsymbol{\sigma}_t\cdot\boldsymbol{\sigma}_t\Big)\,\beta\, d\mathbf{x} + \int_{\Omega\setminus J(\boldsymbol{\xi}_t)} 2\mathsf{d}_1\ell^2 \nabla\alpha_t\cdot\nabla\beta\, d\mathbf{x} \\ + & \int_{\Omega\setminus J(\boldsymbol{\xi}_t)} \sigma_{\mathsf{P}}'(\alpha_t)\bar{p}_t^R\,\beta\, d\mathbf{x} + \int_{J(\boldsymbol{\xi}_t)} \sigma_{\mathsf{P}}'(\alpha_t)\bar{P}_t\,\beta\, dS - \int_{\partial_F\Omega} \mathbf{F}_t\cdot\mathbf{v}\, dS \end{aligned} \tag{38}$$

where the spatial dependence has been dropped and

$$\boldsymbol{\sigma}_t = \mathbb{E}(\alpha_t)(\nabla_s\mathbf{u}_t - \mathbf{p}_t)$$

denotes the stress field at time t. The inequality (38) must hold for all $\mathbf{v}$ such that $\mathbf{v} = \mathbf{0}$ on $\partial_D\Omega$ (and $[\![\mathbf{v}]\!]\cdot\mathbf{n} = 0$ on $J(\mathbf{v})$), all $\beta \geq 0$ and all $\mathbf{q}$ (deviatoric) which satisfies (11). Let us derive the different local conditions which are given by (38).

1. *Equilibrium equations.* Taking first $\beta = 0$, $\mathbf{q} = \mathbf{0}$ and hence $J(\mathbf{v}) = \emptyset$, integrating by parts the gradient of $\mathbf{v}$ term over $\Omega\setminus J(\boldsymbol{\xi}_t)$ and considering that the boundary $\partial(\Omega\setminus J) = \partial\Omega \cup J^+ \cup J^-$ involves both faces (with opposite normals) of the given surface J, one gets:

$$\begin{aligned} \int_{\Omega\setminus J(\boldsymbol{\xi}_t)} \boldsymbol{\sigma}_t\cdot\nabla_s\mathbf{v}\, d\mathbf{x} &= \int_{\partial(\Omega\setminus J(\boldsymbol{\xi}_t))} \boldsymbol{\sigma}_t\mathbf{n}\cdot\mathbf{v}\, d\mathbf{x} - \int_{\Omega\setminus J(\boldsymbol{\xi}_t)} (\nabla\cdot\boldsymbol{\sigma}_t)\cdot\mathbf{v}\, d\mathbf{x} \\ &= \int_{\partial_F\Omega} \boldsymbol{\sigma}_t\mathbf{n}\cdot\mathbf{v}\, d\mathbf{x} - \int_{J(\boldsymbol{\xi}_t)} [\![\boldsymbol{\sigma}_t]\!]\mathbf{n}\cdot\mathbf{v}\, d\mathbf{x} - \int_{\Omega\setminus J(\boldsymbol{\xi}_t)} (\nabla\cdot\boldsymbol{\sigma}_t)\cdot\mathbf{v}\, d\mathbf{x}. \end{aligned} \tag{39}$$

Thus by standard localization arguments one obtains from (38) and (39) the classical equilibrium equations and the natural boundary conditions:

$$\nabla\cdot\boldsymbol{\sigma}_t = \mathbf{0} \text{ in } \Omega\setminus J(\boldsymbol{\xi}_t), \qquad [\![\boldsymbol{\sigma}_t]\!]\mathbf{n} = \mathbf{0} \text{ on } J(\boldsymbol{\xi}_t), \qquad \boldsymbol{\sigma}_t\mathbf{n} = \mathbf{F}_t \text{ on } \partial_F\Omega. \tag{40}$$

Note that the vector stress $\boldsymbol{\sigma}_t\mathbf{n}$ must be continuous on the jump set $J(\boldsymbol{\xi}_t)$ but this is not necessarily true for the other components of the stress tensor. It could happen that $\boldsymbol{\sigma}_t$ is discontinuous across $J(\boldsymbol{\xi}_t)$ and hence not defined on $J(\boldsymbol{\xi}_t)$.

2. *Plasticity yield criterion in the regular part of the domain.* Taking $\mathbf{v} = \mathbf{0}$, $\beta = 0$ and hence $\mathbf{q}^S = \mathbf{0}$, (38) gives

$$\int_{\Omega\setminus J(\boldsymbol{\xi}_t)} \Big(\sigma_{\mathsf{P}}(\alpha_t)k_N\|\mathbf{q}\| - \boldsymbol{\sigma}_t\cdot\mathbf{q}\Big)d\mathbf{x} \geq 0, \qquad \forall\mathbf{q} \text{ smooth}(,\ \mathrm{Tr}\ \mathbf{q} = 0). \tag{41}$$

In the multi-dimensional case, since Tr $\mathbf{q} = 0$, one gets $\boldsymbol{\sigma}_t \cdot \mathbf{q} = \boldsymbol{\sigma}_t^D \cdot \mathbf{q}$ where $\boldsymbol{\sigma}_t^D$ denotes the deviatoric part of $\boldsymbol{\sigma}_t$ and one deduces from (41) that

$$\boldsymbol{\sigma}_t^D \cdot \mathbf{q} \leq k_N \sigma_{\mathsf{P}}(\alpha_t), \quad \forall \mathbf{q} \in \mathbb{M}_s^N \,:\, \mathrm{Tr}\,\mathbf{q} = 0, \|\mathbf{q}\| = 1. \tag{42}$$

This inequality must hold everywhere in $\Omega \setminus J(\boldsymbol{\xi}_t)$ and hence the stress must satisfy:

$$\|\boldsymbol{\sigma}_t^D\| \leq k_N\, \sigma_{\mathsf{P}}(\alpha_t) \quad \text{in} \quad \Omega \setminus J(\boldsymbol{\xi}_t). \tag{43}$$

Thus (43) is actually the standard Von Mises plastic yield criterion obtained as a stability condition associated with the plastic incompressibility hypothesis and the form of the plastic dissipated energy. In the one-dimensional case, one simply deduces from (41) that $|\sigma_t| \leq \sigma_{\mathsf{P}}(\alpha_t)$ in $\Omega \setminus J(\boldsymbol{\xi}_t)$. But since σ_t is a constant and α_t is continuous in space, this inequality must hold everywhere.

3. *Plasticity yield criterion on the jump set $J(\boldsymbol{\xi}_t)$.* Taking $\beta = 0$, $\mathbf{q}^R = \mathbf{0}$, $\mathbf{v}$ such that $J(\mathbf{v}) \neq \emptyset$ and using (40), (38) gives

$$0 \leq \int_{J(\mathbf{v})} \Big(\sigma_{\mathsf{P}}(\alpha_t)\kappa_N \|[\![\mathbf{v}]\!]\| - \sigma_t \mathbf{n} \cdot [\![\mathbf{v}]\!]\Big)\, dS. \tag{44}$$

In the one-dimensional case, since $J(v)$ and $[\![v]\!]$ can be chosen arbitrarily and since $\kappa_N = 1$, one simply re-obtains that $|\sigma_t| \leq \sigma_{\mathsf{P}}(\alpha_t)$ must hold everywhere in Ω.
In the multidimensional case, the jump of $\mathbf{v}$ is restricted by the plastic incompressibility condition, $[\![\mathbf{v}]\!] \cdot \mathbf{n} = 0$ on $J(\mathbf{v})$. Therefore $\sigma_t \mathbf{n} \cdot [\![\mathbf{v}]\!]$ involves the shear stress only and can read as

$$\sigma_t \mathbf{n} \cdot [\![\mathbf{v}]\!] = \big(\sigma_t \mathbf{n} - (\sigma_t \mathbf{n} \cdot \mathbf{n})\,\mathbf{n}\big) \cdot [\![\mathbf{v}]\!].$$

Considering first $\mathbf{v}$ such that $J(\mathbf{v}) \cap J(\boldsymbol{\xi}_t) = \emptyset$ and using the fact that in such a case the direction $\mathbf{n}$ can be chosen arbitrarily, (44) gives the following condition which must hold in $\Omega \setminus J(\boldsymbol{\xi})$:

$$\big(\sigma_t \mathbf{n} - (\sigma_t \mathbf{n} \cdot \mathbf{n})\,\mathbf{n}\big) \cdot \mathbf{t} \leq \kappa_N \sigma_{\mathsf{P}}(\alpha_t), \quad \forall \mathbf{n}, \mathbf{t} \in \mathbb{R}^N \,:\, \|\mathbf{n}\| = \|\mathbf{t}\| = 1, \mathbf{n} \cdot \mathbf{t} = 0.$$

It is easy to see that this condition is equivalent to

$$\max_{\mathbf{n}\,:\,\|\mathbf{n}\|=1} \|\sigma_t \mathbf{n} - (\sigma_t \mathbf{n} \cdot \mathbf{n})\,\mathbf{n}\| \leq \kappa_N \sigma_{\mathsf{P}}(\alpha_t) \quad \text{in} \quad \Omega \setminus J(\boldsymbol{\xi}_t). \tag{45}$$

So, we obtain a maximal shear stress condition which differs from Von Mises plastic yield criterion. In fact this maximal shear stress condition (45) is weaker than Von Mises plastic yield criterion (43) in the sense that (45) is automatically satisfied when (43) holds, but the converse is not true. (The proof of this property is left to the reader.) Accordingly we can disregard (45).
If we consider now $\mathbf{v}$ such that $J(\mathbf{v}) \subset J(\boldsymbol{\xi}_t)$, then the normal vector $\mathbf{n}$ is fixed by $\boldsymbol{\xi}_t$ and (44) gives the following condition on $J(\boldsymbol{\xi}_t)$:

$$\big(\sigma_t \mathbf{n} - (\sigma_t \mathbf{n} \cdot \mathbf{n})\,\mathbf{n}\big) \cdot \mathbf{t} \leq \kappa_N \sigma_{\mathsf{P}}(\alpha_t), \quad \forall \mathbf{t} \in \mathbb{R}^N \,:\, \|\mathbf{t}\| = 1, \mathbf{t} \cdot \mathbf{n} = 0 \tag{46}$$

which is equivalent to

$$\|\sigma_t \mathbf{n} - (\sigma_t \mathbf{n} \cdot \mathbf{n})\,\mathbf{n}\| \leq \kappa_N \sigma_{\mathsf{P}}(\alpha_t) \quad \text{on} \quad J(\boldsymbol{\xi}_t). \tag{47}$$

So, the plasticity yield criterion on the jump set is formulated in terms of the norm of the shear stress vector, what has a sense since the stress vector is well defined on this surface by virtue of (40). Of course, when all the stress tensor field is continuous and hence well defined on $J(\boldsymbol{\xi}_t)$, then Von Mises yield criterion must hold and since it contains the shear stress condition this latter condition can be disregarded. In the doubt we keep (47).

4. *The damage yield criteria.* Taking $\mathbf{v} = \mathbf{0}$ and $\mathbf{q} = \mathbf{0}$, integrating by parts the term in $\nabla\alpha_t \cdot \nabla\beta$, we obtain by classical arguments of Calculus of Variations the following damage yield criteria in the regular part, the singular part and the boundary $\partial\Omega$:

$$\mathsf{d}'(\alpha_t) + \sigma_{\mathsf{P}}'(\alpha_t)\bar{p}_t^R - \tfrac{1}{2}\mathsf{C}'(\alpha_t)\boldsymbol{\sigma}_t \cdot \boldsymbol{\sigma}_t - 2\mathsf{d}_1 \ell^2 \Delta\alpha_t \geq 0 \quad \text{in} \quad \Omega \setminus J(\boldsymbol{\xi}_t) \tag{48}$$

$$\sigma_{\mathsf{P}}'(\alpha_t)\bar{P}_t - 2\mathsf{d}_1 \ell^2 [\![\partial\alpha_t/\partial n]\!] \geq 0 \quad \text{on} \quad J(\boldsymbol{\xi}_t) \tag{49}$$

$$\partial\alpha_t/\partial n \geq 0 \quad \text{on} \quad \partial\Omega. \tag{50}$$

In the case where σ_{P} does not depend on α, we recover the damage yield criteria obtained in Pham and Marigo (2010b); Pham et al. (2011a,b) by the same variational approach and in Comi (1999). But note that here, because of the coupling term between damage and plasticity, the localization of the plastic strain on a surface will in general induce a discontinuity of the damage normal derivative and *vice versa*.

A.2. The plastic flow rules and the consistency equations as consequences of the energy balance

Assuming that the evolution $t \mapsto \boldsymbol{\xi}_t$ is smooth, $t \mapsto \bar{p}_t$ is obtained from $t \mapsto \mathbf{p}_t$ by

$$\dot{\bar{p}}_t^R(\mathbf{x}) = k_N \, \|\dot{\mathbf{p}}_t^R(\mathbf{x})\| \quad \forall \mathbf{x} \in \Omega \setminus J(\boldsymbol{\xi}_t), \qquad \dot{\bar{P}}_t(\mathbf{x}) = \kappa_N \, \|[\![\dot{\mathbf{u}}_t]\!](\mathbf{x})\| \quad \forall \mathbf{x} \in J(\boldsymbol{\xi}_t),$$

where

$$\kappa_N = \begin{cases} 1 & \text{if } N = 1 \\ k_N/\sqrt{2} & \text{otherwise} \end{cases}. \tag{51}$$

Note that $t \mapsto J(\boldsymbol{\xi}_t)$ is not decreasing, *i.e.* the number of singular points can only increase. Indeed, if a jump discontinuity of the displacement appears at a point $\mathbf{x}_s$ at some time t_s, then $\bar{P}_t(\mathbf{x}_s) > 0$ for all $t \geq t_s$. Therefore those points are material points and their position does not depend on time, but their number can increase because new points can appear all along the evolution. Accordingly, using the initial conditions, we can set

$$\bar{p}_t^R(\mathbf{x}) = \int_0^t k_N \, \|\dot{\mathbf{p}}_s^R(\mathbf{x})\| ds, \quad \forall \mathbf{x} \in \Omega \setminus J(\boldsymbol{\xi}_t) \quad \text{and} \quad \bar{P}_t(\mathbf{x}) = \int_0^t \kappa_N \, \|[\![\dot{\mathbf{u}}_s]\!](\mathbf{x})\| ds, \quad \forall \mathbf{x} \in J(\boldsymbol{\xi}_t). \tag{52}$$

Let us now use the energy balance (13). Expanding the time derivative of the total energy, (13) becomes

$$\begin{aligned} 0 \;=\; & \int_{\Omega\setminus J(\boldsymbol{\xi}_t)} \Big(\boldsymbol{\sigma}_t \cdot (\nabla_s \dot{\mathbf{u}}_t - \dot{\mathbf{p}}_t^R) + k_N \sigma_{\mathsf{P}}(\alpha_t) \|\dot{\mathbf{p}}_t^R\| \Big) \, d\mathbf{x} - \int_{\partial_D \Omega} \boldsymbol{\sigma}_t \, \mathbf{n} \cdot \dot{\mathbf{U}}_t \, dS - \int_{\partial_F \Omega} \mathbf{F}_t \cdot \dot{\mathbf{u}}_t \, dS \\ + \; & \int_{\Omega\setminus J(\boldsymbol{\xi}_t)} \Big(-\tfrac{1}{2} \mathsf{C}'(\alpha_t) \boldsymbol{\sigma}_t \cdot \boldsymbol{\sigma}_t \, \dot{\alpha}_t + \mathsf{d}'(\alpha_t) \dot{\alpha}_t + \sigma_{\mathsf{P}}'(\alpha_t) \bar{p}_t^R \dot{\alpha}_t + 2\mathsf{d}_1 \ell^2 \nabla \alpha_t \cdot \nabla \dot{\alpha}_t \Big) \, d\mathbf{x} \\ + \; & \int_{J(\boldsymbol{\xi}_t)} \Big(\sigma_{\mathsf{P}}'(\alpha_t) \bar{P}_t \dot{\alpha}_t + \kappa_N \sigma_{\mathsf{P}}(\alpha_t) \|[\![\dot{\mathbf{u}}_t]\!]\| \Big) \, dS. \end{aligned}$$

Integrating by parts the terms in $\nabla_s \dot{\mathbf{u}}_t$ and $\nabla \dot{\alpha}_t$ above, using the equilibrium equations (40) and the boundary conditions $\dot{\mathbf{u}}_t = \dot{\mathbf{U}}_t$ on $\partial_D \Omega$, the energy balance leads to the following equality

$$\begin{aligned} 0 \;=\; & \int_{\Omega\setminus J(\boldsymbol{\xi}_t)} \Big(k_N \sigma_{\mathsf{P}}(\alpha_t) \|\dot{\mathbf{p}}_t^R\| - \boldsymbol{\sigma}_t \cdot \dot{\mathbf{p}}_t^R \Big) \, d\mathbf{x} + \int_{J(\boldsymbol{\xi}_t)} \Big(\kappa_N \sigma_{\mathsf{P}}(\alpha_t) \|[\![\dot{\mathbf{u}}_t]\!]\| - \boldsymbol{\sigma}_t \mathbf{n} \cdot [\![\dot{\mathbf{u}}_t]\!] \Big) \, dS \\ + \; & \int_{\Omega\setminus J(\boldsymbol{\xi}_t)} \Big(\mathsf{d}'(\alpha_t) + \sigma_{\mathsf{P}}'(\alpha_t) \bar{p}_t^R - \tfrac{1}{2} \mathsf{C}'(\alpha_t) \boldsymbol{\sigma}_t \cdot \boldsymbol{\sigma}_t - 2\mathsf{d}_1 \ell^2 \Delta \alpha_t \Big) \dot{\alpha}_t \, d\mathbf{x} \\ + \; & \int_{J(\boldsymbol{\xi}_t)} \Big(\sigma_{\mathsf{P}}'(\alpha_t) \bar{P}_t - 2\mathsf{d}_1 \ell^2 [\![\frac{\partial \alpha_t}{\partial n}]\!] \Big) \dot{\alpha}_t \, dS + \int_{\partial\Omega} 2\mathsf{d}_1 \ell^2 \frac{\partial \alpha_t}{\partial n} \dot{\alpha}_t \, dS. \end{aligned}$$

1. *The consistency equations.* By virtue of the irreversibility condition (10) and the local first order stability conditions (43), (47), (48)–(50), each of the five integrands above is non negative and hence each must vanish so that their sum be zero. Therefore, we have obtained the three following consistency equations for the damage evolution:

$$\Big(\mathsf{d}'(\alpha_t) + \sigma_{\mathsf{P}}'(\alpha_t) \bar{p}_t^R - \tfrac{1}{2} \mathsf{C}'(\alpha_t) \boldsymbol{\sigma}_t \cdot \boldsymbol{\sigma}_t - 2\mathsf{d}_1 \ell^2 \, \Delta \alpha_t \Big) \dot{\alpha}_t = 0 \quad \text{in} \quad \Omega \setminus J(\boldsymbol{\xi}_t) \tag{53}$$

$$\Big(\sigma_{\mathsf{P}}'(\alpha_t) \bar{P}_t - 2\mathsf{d}_1 \ell^2 [\![\partial \alpha_t / \partial n]\!] \Big) \dot{\alpha}_t = 0 \quad \text{on} \quad J(\boldsymbol{\xi}_t) \tag{54}$$

$$(\partial \alpha_t / \partial n) \, \dot{\alpha}_t = 0 \quad \text{on} \quad \partial\Omega. \tag{55}$$

2. *The plasticity flow rules.* In the multi-dimensional case, the vanishing of the first integrand gives

$$\boldsymbol{\sigma}_t^D \cdot \dot{\mathbf{p}}_t^R = k_N \sigma_{\mathrm{P}}(\alpha_t) \|\dot{\mathbf{p}}_t^R\| \quad \text{in} \quad \Omega \setminus J(\boldsymbol{\xi}_t).$$

But, by virtue of (42) and since $\operatorname{Tr} \dot{\mathbf{p}}_t^R = 0$, the equality above can hold if and only if the normality flow rule for the plastic strain rate holds, *i.e.*

$$\dot{\mathbf{p}}_t^R = \|\dot{\mathbf{p}}_t^R\| \frac{\boldsymbol{\sigma}_t^D}{k_N \sigma_{\mathrm{P}}(\alpha_t)} \quad \text{in} \quad \Omega \setminus J(\boldsymbol{\xi}_t). \tag{56}$$

In the same way, one deduces from the vanishing of the second integrand and $[\![\dot{\mathbf{u}}_t]\!] \cdot \mathbf{n} = 0$ that

$$\big(\sigma_t \mathbf{n} - (\sigma_t \mathbf{n} \cdot \mathbf{n})\, \mathbf{n}\big) \cdot [\![\dot{\mathbf{u}}_t]\!] = \kappa_N \sigma_{\mathrm{P}}(\alpha_t) \|[\![\dot{\mathbf{u}}_t]\!]\| \quad \text{on} \quad J(\boldsymbol{\xi}_t)$$

and hence, by virtue of (46), another normality plastic flow rule on the jump set

$$[\![\dot{\mathbf{u}}_t]\!] = \|[\![\dot{\mathbf{u}}_t]\!]\| \frac{\sigma_t \mathbf{n} - (\sigma_t \mathbf{n} \cdot \mathbf{n})\, \mathbf{n}}{\kappa_N \sigma_{\mathrm{P}}(\alpha_t)} \quad \text{on} \quad J(\boldsymbol{\xi}_t). \tag{57}$$

Note that this latter flow rule is rarely mentioned in the literature and the interest reader can refer to Francfort and Giacomini (2012) where this flow rule is obtained at each interface of an heterogeneous elastic-plastic body.
In the one-dimensional case, these flow rules read as

$$\dot{p}_t^R = |\dot{p}_t^R| \frac{\sigma_t}{\sigma_{\mathrm{P}}(\alpha_t)} \quad \text{in} \quad \Omega \setminus J(\boldsymbol{\xi}_t), \qquad [\![\dot{u}_t]\!] = |[\![\dot{u}_t]\!]| \frac{\sigma_t}{\sigma_{\mathrm{P}}(\alpha_t)} \quad \text{on} \quad J(\boldsymbol{\xi}_t). \tag{58}$$

References

Ambrosio, L., Lemenant, A., Royer-Carfagni, G., 2012. A Variational Model for Plastic Slip and Its Regularization *via* Γ-Convergence. Journal of Elasticity, 1–35.

Amor, H., Marigo, J.-J., Maurini, C., 2009. Variational approach to brittle fracture with unilateral contact: numerical experiments. Journal of the Mechanics and Physics of Solids 57 (8), 1209–1229.

Belnoue, J. P., Nguyen, G. D., Korsunsky, M., 2007. A one-dimensional non local damage-plasticity model for ductile materials. Int. J. Fract. 144, 53–60.

Benallal, A., Marigo, J.-J., 2007. Bifurcation and stability issues in gradient theories with softening. Modelling and Simulation in Materials Science and Engineering 15 (1), S283–S295.

Bourdin, B., Francfort, G. A., Marigo, J.-J., 2000. Numerical experiments in revisited brittle fracture. Journal of the Mechanics and Physics of Solids 48 (4), 797–826.

Bourdin, B., Francfort, G. A., Marigo, J.-J., 2008. The variational approach to fracture. Journal of Elasticity 91 (1–3), 5–148.

Comi, C., 1999. Computational modelling of gradient-enhanced damage in quasi-brittle materials. Mechanics of Cohesive-frictional Materials 4 (1), 17–36.

Comi, C., Mariani, S., Negri, M., Perego, U., 2006. A one-dimensional variational formulation for quasi-brittle fracture. Journal of Mechanics of Materials and Structures 1 (8), 1323–1343.

Dal Corso, F., Willis, J., 2011. Stability of strain-gradient plastic materials. Journal of the Mechanics and Physics of Solids 59 (6), 1251 – 1267.

de Borst, R., Pamin, J., Geers, M. G. D., 1999. On coupled gradient-dependent plasticity and damage theories with a view to localization. European Journal of Mechanics - A/Solids 18, 939–962.

Del Piero, G., 2013. A Variational Approach to Fracture and Other Inelastic Phenomena. J. Elasticity 112 (1), 3–77.

Del Piero, G., Lancioni, G., March, R., 2012. Diffuse cohesive energy in plasticity and fracture. Technische Mechanik 32 (2), 174–188.

Del Piero, G., Truskinovsky, L., 2009. Elastic bars with cohesive energy. Continuum Mechanics and Thermodynamics 21, 141–171.

Dimitrijevic, B. J., Hackl, K., 2011. A regularization framework for damage–plasticity models via gradient enhancement of the free energy. International Journal for Numerical Methods in Biomedical Engineering 27, 1199—1210.

Francfort, G. A., Giacomini, A., 2012. Small-Strain Heterogeneous Elastoplasticity Revisited. Communications on Pure and Applied Mathematics LXV, 1185—1241.

Grassl, P., Jirásek, M., 2006. Plastic model with non-local damage applied to concrete. International Journal for Numerical and Analytical Methods in Geomechanics 30, 71–90.

Lemaitre, J., Chaboche, J., 1985. Mécanique des matériaux solides. Bordas.

Logg, A., Mardal, K., A., W., 2012. Automated Solution of Differential Equations by the Finite Element Method. Springer.

Lorentz, E., Andrieux, S., 2003. Analysis of non-local models through energetic formulations. International Journal of Solids and Structures 40, 2905–2936.

Lorentz, E., Cuvilliez, S., Kazymyrenko, K., 2011. Convergence of a gradient damage model toward a cohesive zone model. Comptes Rendus Mécanique 339 (1), 20 – 26.

Mielke, A., 2005. Evolution of rate-independent systems. Vol. 2 of Handbook of Differential Equations: Evolutionary Equations. North-Holland, pp. 461–559.

Mielke, A., 2006. A mathematical framework for generalized standard materials in the rate-independent case. In: Helmig, R., Mielke, A., Wohlmuth, B. (Eds.), Multifield Problems in Solid and Fluid Mechanics. Vol. 28 of Lecture Notes in Applied and Computational Mechanics. Springer Berlin - Heidelberg, pp. 399–428.

Peerlings, R., de Borst, R., Brekelmans, W., Geers, M., 1998. Gradient-enhanced damage modelling of concrete fracture. Mechanics of Cohesive-frictional Materialsf 3, 323–342.

Pham, K., Amor, H., Marigo, J.-J., Maurini, C., 2011a. Gradient damage models and their use to approximate brittle fracture. International Journal of Damage Mechanics 20 (4), 618–652.

Pham, K., Marigo, J.-J., 2010a. Approche variationnelle de l'endommagement: I. Les concepts fondamentaux. Comptes Rendus Mécanique 338 (4), 191–198.

Pham, K., Marigo, J.-J., 2010b. Approche variationnelle de l'endommagement: II. Les modèles à gradient. Comptes Rendus Mécanique 338 (4), 199–206.

Pham, K., Marigo, J.-J., 2013a. From the onset of damage until the rupture: construction of the responses with damage localization for a general class of gradient damage models. Continuum Mech. Thermodyn. 25 (2–4), 147–171.

Pham, K., Marigo, J.-J., 2013b. Stability of homogeneous states with gradient damage models: size effects and shape effects in the three-dimensional setting. Journal of Elasticity 110 (1), 63–93.

Pham, K., Marigo, J.-J., Maurini, C., 2011b. The issues of the uniqueness and the stability of the homogeneous response in uniaxial tests with gradient damage models. Journal of the Mechanics and Physics of Solids 59 (6), 1163–1190.

Sicsic, P., Marigo, J.-J., 2013. From gradient damage laws to Griffith's theory of crack propagation. J. Elasticity 113 (1), 55–74.

Sicsic, P., Marigo, J.-J., Maurini, C., 2013. Initiation of a periodic array of cracks in the thermal shock problem: a gradient damage modeling. J. Mech. Phys. Solids http://dx.doi.org/10.1016/j.jmps.2013.09.003.